

SIMULATION OF FREQUENCY SELECTIVE FADING CHANNELS

SASHI KANTH DHARMANNOLA

Department of Electrical and Computer Engineering

APPROVED:

Bryan E. Usevitch, Ph.D., Chair

Scott A. Starks, Ph.D.

Kallol K. Bagchi, Ph.D.

Pablo Arenaz, Ph.D.
Dean of the Graduate School

Dedicated to
my parents

SIMULATION OF FREQUENCY SELECTIVE FADING CHANNELS

by

SASHI KANTH DHARMANNOLA

THESIS

Presented to the Faculty of the Graduate School of

The University of Texas at El Paso

in Partial Fulfillment

of the Requirements

for the Degree of

MASTER OF SCIENCE

Department of Electrical and Computer Engineering

THE UNIVERSITY OF TEXAS AT EL PASO

July 2006

UMI Number: 1460432

INFORMATION TO USERS

The quality of this reproduction is dependent upon the quality of the copy submitted. Broken or indistinct print, colored or poor quality illustrations and photographs, print bleed-through, substandard margins, and improper alignment can adversely affect reproduction.

In the unlikely event that the author did not send a complete manuscript and there are missing pages, these will be noted. Also, if unauthorized copyright material had to be removed, a note will indicate the deletion.



UMI Microform 1460432
Copyright 2009 by ProQuest LLC
All rights reserved. This microform edition is protected against
unauthorized copying under Title 17, United States Code.

ProQuest LLC
789 East Eisenhower Parkway
P.O. Box 1346
Ann Arbor, MI 48106-1346

Acknowledgements

I would like to sincerely thank my advisor, Dr. Bryan E. Usevitch, for his continuous support, encouragement and invaluable insights.

Sincere thanks to my committee members Dr. Stark A. Starks, Dr. Kallol K. Bagchi for their valuable time and suggestions. Their honest yet considerate criticism of this work helped me much in improving my work.

I thank one and all in the faculty and staff of the Electrical and Computer Engineering Department, friends at the Signal Processing and Communications Lab Pedro, Ramani, Aldo for their help and support.

I thank my roommates Ravi, Mitra, Rama Krishna, Siva and Riddhish for their continuous support. I would like to thank Gopi Manne for his help on LATEX, Vikram Jayaram for many hours of discussions (most of them were less related to my thesis!). I express my deepest gratitude to Texas Instruments Foundation, for supporting my education.

Finally, I would like to express my gratitude to my family members, for everything they provided. Without their help and support, I couldn't have completed my studies. Lastly but certainly not the least, I thank the Almighty for everything.

This thesis was presented to the committee on July 21st, 2006.

Abstract

In wireless communications the received electromagnetic wave is distorted due to the presence of multiple replicas of the transmitted wave present at the receiver antenna and this effect is known as multipath fading. This effect has to be studied to develop communication techniques which can effectively mitigate the distortions introduced into the transmitted signal by the wireless channel. To study the effect of multipath fading in wireless communication systems, the more cost effective and flexible way is to develop computer simulation models.

In this thesis, we model frequency-selective multipath channels, for different propagation environments specified by COST 207. To develop an efficient computer simulation model which approximates the various multipath propagation environments specified by COST 207 we used the deterministic simulation approach given in [1]. A computer simulation model is developed in MATLAB, which approximates the statistical characteristics of the reference model. The developed simulation model is useful for studying the effects of multipath fading channels and can be used to study the effectiveness of various communication techniques in multipath channels. The simulation model is developed as a MATLAB function which can be used in other simulation programs. The scattering function which gives valuable information about the channel is generated according to COST 207 specifications.

Table of Contents

	Page
Acknowledgements	iv
Abstract	v
Table of Contents	vi
List of Tables	viii
List of Figures	ix
Chapter	
1 Introduction	1
1.1 Wireless Channel Basics	1
1.2 Linear Time-Varying Systems	5
1.2.1 Time-Domain Representation of Linear Time-Varying systems	5
1.2.2 The Superposition Integral	6
1.2.3 Frequency-Domain Representation of Linear-Time Varying Systems . .	7
1.3 Motivation	8
Chapter	
2 Fading Multipath Channels	10
2.1 Introduction	10
2.2 Charecterization of Multipath Channels	11
2.2.1 Envelope and Phase Distribution of the Received Signal	12
2.3 Statistical Characterization of Multipath Channels	14
2.3.1 Power Delay Profile	16
2.3.2 Spaced-Frequency Correlation Function:	19
2.3.3 Doppler power spectrum:	20
2.3.4 Spaced-Time Correlation Function:	21
Chapter	

3	Methods for Simulation of Multipath-Fading Channels	24
3.1	Introduction	24
3.2	Deterministic Channel Modeling	25
3.2.1	Filter Method	25
3.2.2	Rice Method	26
3.3	Properties of Deterministic Processes	29
3.4	Methods to Compute the Model Parameters for Deterministic Processes . . .	32
3.4.1	Method of Equal Areas (MEAS)	33
3.4.2	Method of Exact Doppler Spread (MEDS)	37
3.4.3	Doppler Phase Coefficients	42
Chapter		
4	Frequency Selective Channel Models	46
4.1	COST 207 Channel Models	48
4.2	Deterministic Frequency Channel Models	53
4.3	Autocorrelation Function and Power Spectral Density	58
4.4	Determination of Model Parameters	59
Chapter		
5	Simulation Results	63
5.1	Results	67
5.2	Conclusion and Future Work	79
Bibliography		81
Curriculum Vitae		83

List of Tables

List of Figures

1.1	A mobile wireless channel environment illustrating the multipath propagation	3
1.2	A plane wave incident on a mobile station	4
2.1	Response of a linear time-varying discrete mulitpath channel to a short dura- tion pulses.	13
2.2	The Power Delay Profile.	17
2.3	The Spaced-Frequency Correlation Function.	20
2.4	Doppler power spectrum.	21
2.5	The Spaced-Time Correlation Function.	22
3.1	Filter method to model a colored Gaussian random process.	25
3.2	Rice method to model a colored Gaussian random process.	26
3.3	Deterministic simulation model for coloured Gaussian random processes [1]. .	29
3.4	Power spectral density $\tilde{S}_{\mu\mu}(f)$ for $N = 14$, $f_m = 100$, $\sigma_0^2 = 1$ (MEAS, Jakes psd).	35
3.5	Autocorrelation function $\tilde{r}_{\mu\mu}(\tau)$ for $N = 14$, $f_m = 100$, $\sigma_0^2 = 1$ (MEAS, Autocorrelation function).	36
3.6	Power spectral density $\tilde{S}_{\mu\mu}(f)$ for $N = 14$, $f_m = 100$, $\sigma_0^2 = 1$ (MEDS, Jakes psd).	39
3.7	Autocorrelation function $\tilde{r}_{\mu\mu}(\tau)$ for $N = 14$, $f_m = 100$, $\sigma_0^2 = 1$ (MEDS, Autocorrelation function).	40
3.8	Autocorrelation function $\tilde{r}_{\mu\mu}(\tau)$ for $N = 25$, $f_m = 100$, $\sigma_0^2 = 1$ (MEDS, Autocorrelation function).	41
3.9	Influence of $\theta_{i,n}$ on the behavior of $\tilde{\zeta}(t)$: $\theta_{i,n} \in (0, 2\pi]$	43
3.10	Influence of $\theta_{i,n}$ on the behavior of $\tilde{\zeta}(t)$: $\theta_{i,n} = 0$	44
3.11	Influence of $\theta_{i,n}$ on the behavior of $\tilde{\zeta}(t)$: Permuted phases.	45

4.1	Bajwa and Parsons Ellipses Model to describe the multipath signal path geometry [1], [16].	47
4.2	Delay power spectral density $S_{\tau'\tau'}(\tau')$ for Rural Area (RA).	49
4.3	Delay power spectral density $S_{\tau'\tau'}(\tau')$ for Typical Urban (TU).	50
4.4	Delay power spectral density $S_{\tau'\tau'}(\tau')$ for Bad Urban Area (BU).	51
4.5	Delay power spectral density $S_{\tau'\tau'}(\tau')$ for Hilly Terrain Area (HT).	52
4.6	Tapped delay line model for a frequency channel model.	56
5.1	The Multipath Power Delay Profile $\tilde{S}_{\tau'\tau'}(\tau')$ of a Typical Urban power delay profile	64
5.2	The Multipath Power Delay Profile $\tilde{S}_{\tau'\tau'}(\tau')$ of a Rural Area (RA) power delay profile	65
5.3	The time-variant impulse response of a frequency selective channel.	67
5.4	The Autocorrelation function $\tilde{r}_{\tilde{\mu}\tilde{\mu}}(\tau')$ of Rural Area propagation model. . . .	68
5.5	The Scattering function $\tilde{S}(\tau', f)$ of Rural Area propagation model.	69
5.6	The Jakes power spectral density $\tilde{S}_{\tilde{\mu}\tilde{\mu}}(f)$ of Rural Area propagation model. .	70
5.7	The Power Delay Profile $\tilde{S}_{\tau'\tau'}(\tau')$ of Rural Area propagation model.	71
5.8	The Scattering function $\tilde{S}(\tau', f)$ of Typical Urban Area propagation model. .	72
5.9	The Jakes power spectral density $\tilde{S}_{\tilde{\mu}\tilde{\mu}}(f)$ of Typical Urban Area propagation model.	73
5.10	The Power Delay Profile $\tilde{S}_{\tau'\tau'}(\tau')$ of Typical Urban Area propagation model.	74
5.11	The Scattering function $\tilde{S}(\tau', f)$ of Bad Urban Area propagation model. . . .	75
5.12	The Jakes power spectral density $\tilde{S}_{\tilde{\mu}\tilde{\mu}}(f)$ of Bad Urban Area propagation model.	76
5.13	The Power Delay Profile $\tilde{S}_{\tau'\tau'}(\tau')$ of Bad Urban Area propagation model. . .	77
5.14	The Scattering function $\tilde{S}(\tau', f)$ of Hilly Terrain propagation model.	78
5.15	The Jakes power spectral density $\tilde{S}_{\tilde{\mu}\tilde{\mu}}(f)$ of Hilly Terrain propagation model.	79
5.16	The Power Delay Profile $\tilde{S}_{\tau'\tau'}(\tau')$ of Hilly Terrain propagation model. . . .	80

Chapter 1

Introduction

Modern communication channels include twisted pairs of wires, coaxial cable, optical fibers, and wireless communication channels and all the modern communication systems operate over the above given channels. Irrespective of the medium of propagation (or channel) used there is some distortion, noise, and interference introduced into the received signal. The effects of the channel can be mitigated by appropriate modulation, coding and other signal-processing techniques like equalization. The communication receiver design becomes complicated in case of wireless channels as they introduce significant levels of interference, distortion, and also noise.

Spectrally efficient wireless communication systems design requires detailed understanding of the wireless propagation environment. The mode of propagation and operating frequency have an effect on the characteristics of a wireless propagation environment also known as the wireless channel. The detailed understanding of the wireless channel helps to answer some of the open questions, example, how to utilize the existing resources (power, available frequency range) economically cater to increasing number of subscribers and also helps to understand the reliability and security of data transmission provided to the subscriber at an affordable price and without involving complicated systems.

1.1 Wireless Channel Basics

Emitted radio waves in a wireless propagation environment reach the receiver often in indirect paths due to various objects blocking the direct path also known as line-of-sight path

between the receiver and transmitter. The electromagnetic wave is reflected in all directions due to various obstacles like trees, buildings, vehicles and other obstacles. The received wave is not only reflected from the surface of the obstacle but it has also the effects of refraction and scattering. The received wave is a superposition of all the waves at the receiver and this effect is known as *multipath propagation*. Figure 1.1 shows the typical multipath propagation environment.

The multipath effect causes the received signal to consist of a sum of infinite number of amplitude attenuated, time delayed and phase-shifted signals which are replicas of the original transmitted signal, each signal effects the other signals. The signals received at the receiver can be constructive or destructive and it depends on the phase-shift experienced by each replica of the original wave. The other effects of the multipath apart from the constructive or destructive superposition occurs when digital signals are transmitted. The transmitted impulses are distorted and at the receiver several individual impulses occur and this effect is called the *impulse dispersion*.

The wireless channels have another effect known as *Doppler effect* this occurs due to the movement of the mobile unit. Doppler effect also has a very negative influence on the wireless channel transmission characteristics. As said earlier the doppler effect is due to the movement of mobile unit or receiver and causes the frequency shift of each of the delayed transmitted waves. The Figure 1.2 shows a horizontal x - y plane, the mobile station (MS) moving along the x -axis with a velocity v .

The n th incident wave arrives at the MS antenna with an angle of incidence α_n . Due to the MS movement a frequency shift or **Doppler** shift is introduced into the incident wave. The amount of Doppler shift introduced into the incident wave is given by [1],

$$f_n = f_m \cos \alpha_n \quad (1.1)$$

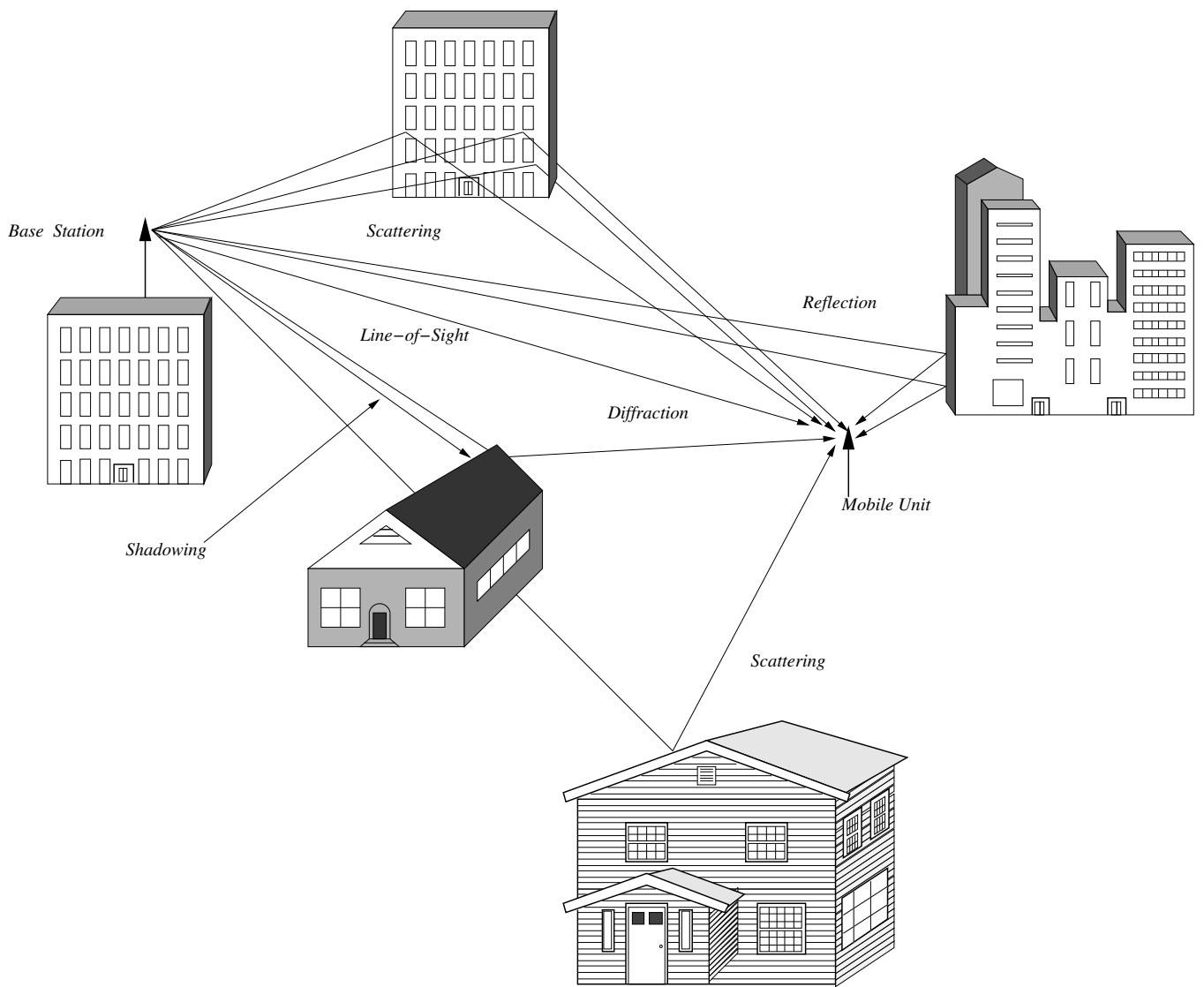


Figure 1.1: A mobile wireless channel environment illustrating the multipath propagation

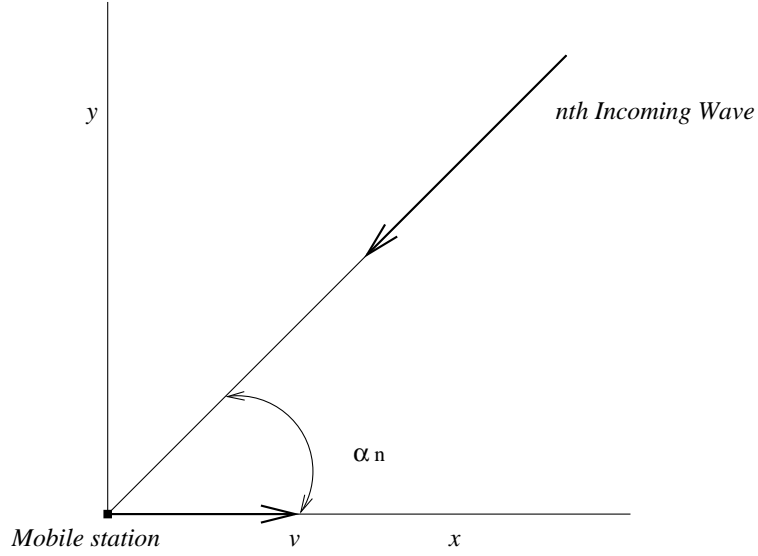


Figure 1.2: A plane wave incident on a mobile station

where f_m is the *maximum Doppler frequency* it is related to the velocity v of the MS and is given by [1],

$$f_m = \frac{v}{c} f_c \quad (1.2)$$

The maximum doppler frequency occurs when $\alpha_n = 0$. The incident waves arriving opposite in direction of the MS movement experience negative doppler shift and the waves arriving in the same direction experience positive Doppler shift.

Multipath propagation combined with the receiver or transmitter movement leads to large level of degradation of the received signal due to drastic and random fluctuations. Due to the random fluctuations in the received signal, Fades of 30 to 40dB or even below the mean value of the received signal can occur. Figure 1.3 depicts the behavior of a signal received in wireless communications. In this example the speed of MS is assumed to be $v = 100Km/h$ and the carrier frequency $f_c = 950MHz$. The maximum doppler frequency according to (1.2) comes out to be $f_m = 88Hz$.

1.2 Linear Time-Varying Systems

A communication system consisting of linear elements may be time-invariant or time-varying in nature. The time invariance property of a linear system implies that the modeled system properties do not change over (long periods of) time. The time-invariant transfer function remains fixed and does not change as a function of time. To classify a system as time-invariant or time-variant usually depends on how fast the characteristics of systems being modeled are changing in comparison to other parameters of the system such as symbol rate. If the symbol rate of the system is very small compared to the time constant associated with the time variations the system can be modeled as a time-invariant system. If the time constant associated with the time variations is at a rate approaching the symbol rate of the communication system then the system can be modeled as a time-varying system. In this section we review the basics of linear-time varying systems.

1.2.1 Time-Domain Representation of Linear Time-Varying systems

The impulse response of the linear-time varying system is modeled on the definition of linear time-invariant impulse response which is defined as [2]

$$h(t - \tau) = \gamma[\Delta(t - \tau)] \quad (1.3)$$

where the function $h(t)$ is called the impulse response of a linear system to a delta function $\Delta(t)$ and is defined as [2]:

$$h(t) = \gamma[\Delta(t)] \quad (1.4)$$

From Equation (1.3) the impulse response of a linear time-varying system is defined as [2]:

$$h(t, \tau) = \gamma[\Delta(t - \tau)] \quad (1.5)$$

where τ is the time when the impulse response is applied and γ is the linear time-varying system operator.

Linear time-varying system models are used in communication systems in modeling multipath channels as they are time-varying. The behavior of such channels is described by several alternative formulations for the impulse response, but one formulation which is more convenient for modeling communication channels is given by [2],

$$c(\tau, t) = \gamma[\Delta(t - (t - \tau))] = \gamma[\Delta(\tau)] \quad (1.6)$$

Equation (1.6) is known as the channel impulse response (CIR). The relation between the impulse response and CIR is $c(\tau, t) = h(t, t - \tau)$ or $h(t, \tau) = c(t - \tau, t)$. The impulse response will change as a function of both time at which the impulse is applied and at the time at which the output is measured as the system is time-varying.

For the system to be causal the impulse response $h(t, \tau) = 0$ for $t < \tau$ and from the relationship $c(\tau, t) = h(t, t - \tau)$ and $\tau = t - \tau$, a simple correspondence can be established between the two functions.

1.2.2 The Superposition Integral

The superposition integral is used to determine the response of the system to an arbitrary input applied to the system. The response of the system using the superposition integral is given by [2],

$$y(t) = \int_{-\infty}^{+\infty} h(t, \tau) x(\tau) d\tau$$

or

$$y(t) = h(t, \tau) * x(\tau) \quad (1.7)$$

The Equation (1.7) in terms of CIR can be written as [2]:

$$y(t) = \int_{-\infty}^{+\infty} c(\tau, t) x(t - \tau) d\tau$$

or

$$y(t) = c(\tau, t) * x(t - \tau) \quad (1.8)$$

If the system is linear time-invariant then the Equation (1.8) is convolution integral because $h(t, \tau) = h(t - \tau)$ and $c(\tau, t) = c(\tau)$. For causal systems the Equation (1.7) can be written as

$$y(t) = \int_{-\infty}^t h(t, \tau)x(\tau)d\tau \quad (1.9)$$

because for causal systems $h(t, \tau) = 0$ for $t < \tau$ and the response of system in terms of CIR is given by ,

$$y(t) = \int_0^{\infty} c(\tau, t)x(t - \tau)d\tau \quad (1.10)$$

where $c(\tau, t) = 0$ for $\tau < 0$ for causal systems.

1.2.3 Frequency-Domain Representation of Linear-Time Varying Systems

This section describes the frequency-domain representation of the linear time-varying systems. The transfer function for a linear time-varying system can be obtained by taking the fourier transform of the $c(\tau, t)$ with respect to τ and it is denoted as $C_{\tau}(f, t)$ this is a time-varying transfer function [2],

$$C_{\tau}(f, t) = \int_{-\infty}^{+\infty} c(\tau, t)e^{-j2\pi f\tau}d\tau \quad (1.11)$$

$C_{\tau}(f, t)$ and $c(\tau, t)$ have a common variable t in them indicating that they are time-varying. A rapidly time-varying system is one which has fast changes associated with t . The inverse transform is given by [2],

$$c(\tau, t) = \int_{-\infty}^{+\infty} C_{\tau}(f, t)e^{j2\pi f\tau}df \quad (1.12)$$

and output $y(t)$ of the system $c(\tau, t)$, to an arbitrary input $x(t)$ can be determined by [2],

$$y(t) = \int_{-\infty}^{+\infty} C_{\tau}(f, t)X(f)e^{2\pi ft}df \quad (1.13)$$

where $X(f)$ is the Fourier transform of the arbitrary input signal $x(t)$.

Consider the Fourier transform of the CIR $c(\tau, t)$ represented as $C_{\tau}(f, t)$, now by taking the Fourier transform of this function with respect to t gives a two-dimensional frequency response $C_{\tau,t}(f, v)$ which is given by [2],

$$\begin{aligned} C_{\tau,t}(f, v) &= \int_{-\infty}^{+\infty} C_{\tau}(f, t) e^{-j2\pi vt} dt \\ &= \int_{-\infty}^{+\infty} \int_{-\infty}^{+\infty} c(\tau, t) e^{-j2\pi f\tau} e^{-j2\pi vt} d\tau dt \end{aligned} \quad (1.14)$$

the frequency f is associated with the system excitation frequency and the frequency v is associated with rate of change of the system. From the Equation (1.13) and (1.14) the frequency response of the system output can be calculated by [2],

$$Y(v) = \int_{-\infty}^{+\infty} C_{\tau,t}(f, v - f) X(f) df \quad (1.15)$$

The Equation (1.15) is the convolution of frequency response of input $X(f)$ and the system frequency-domain characteristics $C_{\tau,t}(f, v)$ in frequency domain.

1.3 Motivation

As mentioned before in earlier sections, in wireless communication channels the multipath effect is caused by the multiple replicas of the transmitted signal that arrive at the receiver from different paths due to various obstacles blocking the path of the transmitted signal. Due to this, fading and multipath effects can be extremely destructive and introduces intersymbol interference (ISI) in the received signal. To achieve reliable communications over multipath channel, the effects of the channel on the transmitted signal needs to be studied to develop techniques which can effectively mitigate the various distortions introduced into the transmitted signal by the channel. The channel effects can be studied by doing real tests and also by developing hardware simulation models. The former method is very expensive and the latter is not so flexible to implement. The more cost effective and flexible way is to develop software simulated computer models which can be used to study the effects of the channel. This thesis work concentrates on developing an efficient computer simulation model

using **MATLAB**, based on the theory of deterministic processes. The simulation model tries to approximate the characteristics of the multipath channel and so may not present a very realistic view of the fading phenomenon which is complex and random in nature. The simulation model is useful for research work to study the effectiveness of various communication techniques in multipath channels. The simulation model is developed as a **MATLAB** function which can be readily plugged into other simulation programs. The model can be reused to simulate various propagation environments according to **COST 207** [4] specifications developed based on wide-sense stationary uncorrelated scattering (**WSSUS**) assumption. The **COST 207** specifications and various propagation environments are defined and also **WSSUS** assumption is explained in detail in latter chapters.

Chapter 2

Fading Multipath Channels

2.1 Introduction

Wireless communication channels very often introduce fading and multipath effects into the transmitted signal. The transmitted signal has more than one path over which the transmitted signal can reach the receiver. The multiple paths occur due to scattering and reflections from various objects like buildings, trees and other high raising structures that block the line of sight path between transmitter and receiver. In multipath environments the signals that arrive by different paths have different attenuation levels and delays and they are random in nature. These multipath signals with different attenuation levels and random phase combine at the receiver to give a resultant signal with random fluctuations and these random fluctuations in the received signal are called *fading*.

The multipath fading is also known as the *small-scale fading*, in addition to this effect there is another type of fading known as *shadowing* or *large scale fading*. The *shadowing* effect as the name suggests is caused by the high raise buildings and hills standing in between the transmitter and receiver, where the receiver is *shadowed* by these obstacles. *Shadowing* results in attenuation of the received signal power. The multipath fading channels can be divided into categories depending on the number of multipath components reaching the receiver [2].

- If the multipath signal consists of a finite number of multipath components then the channel is known as a *discrete multipath channel*.
- If the multipath signals consists of infinite number of unresolvable multipath compo-

nents then the channel is known as a *diffuse multipath channel*.

2.2 Charecterization of Multipath Channels

Consider a band pass signal $x(t)$ transmitted over a multipath fading channel compromised of N different propagation paths. The band pass signal $x(t)$ represented in its low pass equivalent form is given by

$$x(t) = \text{Re}\{\tilde{x}(t)e^{j2\pi f_c t}\}, \quad (2.1)$$

where $\tilde{x}(t)$ represents the complex envelope of the transmitted signal $x(t)$, f_c represents the carrier frequency, and $\text{Re}[\cdot]$ represents the real part of a complex number. The received signal $y(t)$ is given by [2]

$$y(t) = \sum_{n=1}^N a_n(t)x(t - \tau_n(t)), \quad (2.2)$$

where $a_n(t)$ represents the amplitude attenuation associated with each path and $\tau_n(t)$ represents the time delay associated with each path. The amplitude attenuation magnitude depends on the reflecting surface cross section area. Substituting the (2.1) into (2.2) the output $y(t)$ can be written as

$$\begin{aligned} y(t) &= \text{Re}\left\{\sum_{n=1}^N a_n(t)\tilde{x}(t - \tau_n(t))e^{j2\pi f_c(t - \tau_n(t))}\right\} \\ &= \text{Re}\left\{\left[\sum_{n=1}^N a_n(t)\tilde{x}(t - \tau_n(t))e^{-j2\pi f_c \tau_n(t)}\right]e^{j2\pi f_c t}\right\}. \end{aligned} \quad (2.3)$$

The received signal $y(t)$ can be represented in its low pass equivalent representation given by

$$y(t) = \text{Re}\{\tilde{y}(t)e^{j2\pi f_c t}\}, \quad (2.4)$$

where $\tilde{y}(t)$ represents the complex envelope of the received signal and can be obtained by comparing (2.3) and (2.4) and is given by

$$\tilde{y}(t) = \sum_{n=1}^N a_n(t)\tilde{x}(t - \tau_n(t))e^{-j2\pi f_c \tau_n(t)}. \quad (2.5)$$

The low pass equivalent multipath channel impulse response $h(\tau, t)$ is obtained from (2.5) and is given by [2]

$$h(\tau, t) = \sum_{n=1}^N \tilde{a}_n(\tau_n(t), t) \delta(t - \tau_n(t)), \quad (2.6)$$

where $\tilde{a}_n(\tau(t), t)$ is the low pass equivalent of the signal attenuation associated with the n th path and is given by [2]

$$\sum_{n=1}^N \tilde{a}_n(\tau_n(t), t) = \sum_{n=1}^N a_n(t) e^{-j2\pi f_c \tau_n(t)}. \quad (2.7)$$

The channel impulse is complex and time varying in nature and can be modeled as a time-varying linear filter with the impulse response given by (2.6) and is defined as the impulse response of a system to an input applied at time $t - \tau$ and measured at a time t .

The multipath fading channels effect on the transmitted signal results in the time spreading of the symbol duration in a received signal and also the channel is time-varying because of the relative motion between the receiver and transmitter. The Figure 2.1 shows the effects of the discrete channel on the transmitted short duration pulses.

2.2.1 Envelope and Phase Distribution of the Received Signal

To model the random fluctuations in the received signal introduced by the multipath fading channels the channel impulse response $h(\tau, t)$ is treated as a random process in time t . The multipath signals are formed by summation of an infinite number of scattered and reflected waves from the surfaces of various objects like buildings, hills and other objects that block the path between the transmitter and receiver, the multipath signals can be modeled as complex gaussian random variables by virtue of *central limit theorem* which states that probability distribution function of the sum of infinite number of random variables is gaussian distributed irrespective of the underlying random variables individual distribution functions. The multipath signal is complex gaussian random variable i.e., at any time the real and

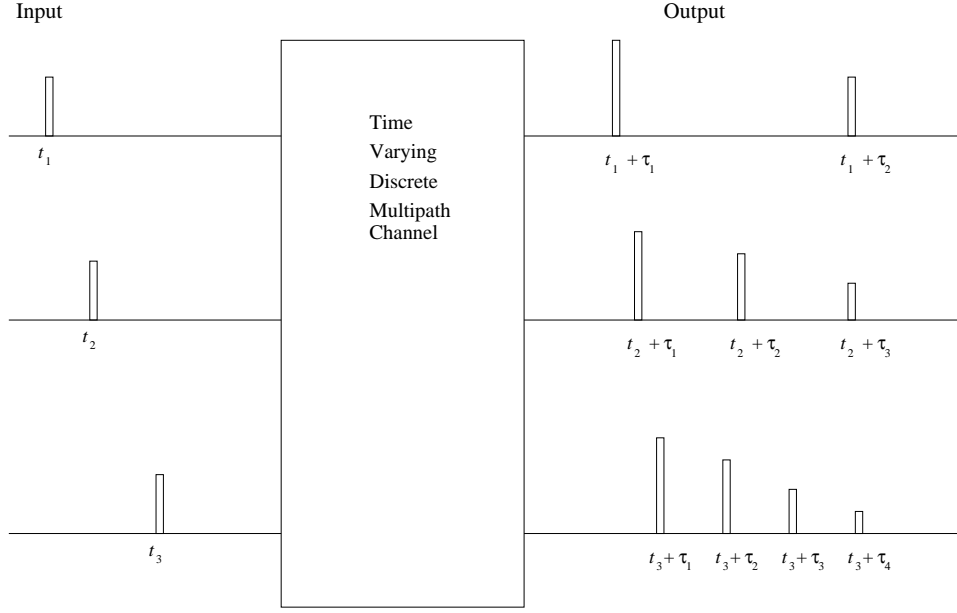


Figure 2.1: Response of a linear time-varying discrete multipath channel to a short duration pulses.

imaginary parts are Gaussian. At each delay time τ the multipath signal consists of infinite number of unresolvable components.

The received channel impulse response envelope takes the *Rayleigh probability density function* if the received signal has no line-of-sight component and is given by

$$f_R(r) = \frac{r}{\sigma_0^2} e^{-\left(\frac{r^2}{2\sigma_0^2}\right)}, \quad r > 0, \\ = 0, \quad r < 0. \quad (2.8)$$

If the received channel impulse response has a nonzero mean i.e., if it has a line of sight component then the received envelope can be modeled as a *Rice probability density function* given by [2]

$$f_R(r) = \frac{r}{\sigma_0^2} e^{-\left(\frac{r^2 + A^2}{2\sigma_0^2}\right)} I_0\left(\frac{Ar}{\sigma_0^2}\right), \quad r > 0, \\ = 0, \quad r < 0, \quad (2.9)$$

where the $I_0(\cdot)$ is the zeroth-order modified bessel function and A represents the nonzero

mean of the received signal.

The random phase associated with the doppler shift in the multipath fading channels takes the *uniform probability density function* given by

$$\begin{aligned} f_{\Theta}(\theta) &= \frac{1}{2\pi}, & \text{if } \theta \in [-\pi, \pi), \\ &= 0, & \text{else.} \end{aligned} \quad (2.10)$$

2.3 Statistical Characterization of Multipath Channels

The multipath fading channel is a random linear time-varying system and can be accurately modeled if treated as a random time-varying filter with impulse response $h(\tau, t)$ given by (2.6) and is defined as the channel impulse measured at a time t to an impulse applied at a time $t - \tau$. The impulse response $h(\tau, t)$ is treated as a random process in time t and different multipath signals for each delay time τ are the sample functions of the random process. The *autocorrelation function* denoted as $R_{hh}(\tau_1, \tau_2; t_1, t_2)$ and is defined as

$$R_{hh}(\tau_1, \tau_2; t_1, t_2) = E\{h^*(\tau_1, t_1)h(\tau_2, t_2)\}, \quad (2.11)$$

where $E\{\cdot\}$ represents the expected value and $h^*(\tau, t)$ represents the complex conjugate of the channel impulse response.

WSS Channel Models: If the impulse response of a channel model is wide-sense stationary i.e., the channel impulse response is independent of time t , then the channel is called *wide-sense stationary channel model* or simply *WSS channel model*. The *autocorrelation function* $R_{hh}(\tau, t)$ is independent of time t , because of *WSS model* assumption and it depends on the time difference δt given by $\Delta t = t_2 - t_1$, where $t_2 = t + \Delta t$ and $t_1 = t$, the *autocorrelation function* for *WSS channel models* is given by

$$R_{hh}(\tau_1, \tau_2, \Delta t) = E\{h^*(\tau_1, t)h(\tau_2, t + \Delta t)\}. \quad (2.12)$$

US Channel Models: The *uncorrelated scattering* condition is obtained by assuming the scattering components with different n th path signals are statistically uncorrelated for different propagation delays. These channel models are known as *uncorrelated scattering channel models* or simply *US models*. The *autocorrelation function* $R_{hh}(\tau_1, \tau_2; t_1, t_2)$ for the *US channel* assumption is given by

$$R_{hh}(\tau_1, \tau_2; t_1, t_2) = R_{hh}(\tau_1; t_1, t_2)\delta(\tau_1 - \tau_2), \quad (2.13)$$

where $\delta(\cdot)$ represents the *Dirac delta function*.

WSSUS Channel Models: The WSSUS channel models form the most important channel models represented by the models belonging to both *WSS channel models* and *US channel models*. The resultant channel models with wide-sense stationary impulse responses and uncorrelated scattering multipath components are popularly known as *wide-sense stationary uncorrelated scattering channel models* or *WSSUS models*. The *autocorrelation function* is denoted as $R_{hh}(\tau, \Delta t)$ and is given by [2]

$$R_{hh}(\tau, \Delta t) = E\{h^*(\tau, t)h(\tau, t + \Delta t)\}. \quad (2.14)$$

The WSSUS channel models with *autocorrelation function* given by (2.14) can be represented in the frequency domain by performing a Fourier transform on one or both variables t and τ . One representation which provides a general description of the channel properties with respect to delay time τ in time domain and the doppler frequency f in frequency domain simultaneously is obtained by performing a Fourier transform on the variable Δt is denoted as $S(\tau, f)$ is called the *scattering function* and is given by

$$S(\tau, f) = \int_{-\infty}^{\infty} R_{hh}(\tau, \Delta t)e^{-j2\pi f\Delta t}d\Delta t. \quad (2.15)$$

The *scattering function* $S(\tau, f)$ is a function of two variables, frequency domain variable f and time domain variable, delay time τ . The scattering function of a channel provides the

average power output as a function of delay time τ and the Doppler frequency f .

The scattering function gives two important relationships of a channel, which effect the performance of a communication system using that channel. The important relationships that can be derived from the scattering function are *power delay profile* and *Doppler power spectrum*. The *power delay profile* also known as the *multipath intensity profile* gives the distribution of average received power as a function of delay time. The *power delay profile* denoted as $p(\tau)$ and is defined as [2]

$$p(\tau) = R_{hh}(\tau, 0) = E|h(\tau, t)|^2 \quad (2.16)$$

The *power delay profile* $p(\tau)$ can be obtained from the *scattering function* through the relation given below

$$p(\tau) = \int_{-\infty}^{\infty} S(\tau, f) df \quad (2.17)$$

The second important function useful in fading characterization known as *Doppler power spectrum* is derived from the scattering function through the relation given by

$$S(f) = \int_{-\infty}^{\infty} S(\tau, f) d\tau \quad (2.18)$$

The *power delay profile* $p(\tau)$ and its Fourier transform denoted as $P(\Delta v)$ and is known as *spaced-frequency correlation function* along with the *Doppler power spectrum* $S(f)$ and its inverse Fourier transform known as *spaced-time correlation function* and denoted as $\rho(\Delta\tau)$ are very important for channel behavior characterization. A detailed description of the four functions is given below.

2.3.1 Power Delay Profile

The power delay profile gives an estimate of the average power of a multipath power measured from the first signal that arrives at the receiver to the last component whose power level is below some threshold level and it is a function of the delay time τ . Figure 2.2 shows an example power delay profile. The *maximum delay spread* also termed as *maximum excess*

delay and denoted as T_m is the difference between the first and last component of the signal whose power level is above a given threshold level. A channel can be classified as frequency selective or frequency nonselective depending on the relationship between the *maximum delay spread* T_m and the symbol time period T_{sym} .

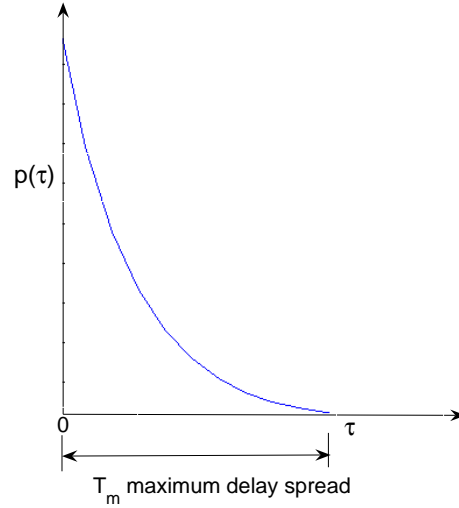


Figure 2.2: The Power Delay Profile.

- A channel can be considered as a frequency selective channel if $T_m > T_{sym}$. If the channel is frequency selective then it introduces intersymbol interference (ISI) distortion into the signal. The ISI effect can be mitigated using equalization at the receiver and this is possible, due to the fact that multipaths are resolvable in the frequency selective channel.
- A channel is considered as a frequency nonselective if $T_m < T_{sym}$. A frequency nonselective channel introduces very little *ISI*, but the distortion still exists in the system,

this is due to the fact that a multipath signal can add destructively, resulting in signal-to-noise ratio (SNR) reduction. To mitigate the effects of a frequency nonselective channel the counter measure technique used is either power control or diversity.

The multipath signal components arrive in a short fraction of time in case of a frequency nonselective channel and can be modeled by a single ray. The input/output relation in the case of a frequency nonselective channel can be expressed as a multiplication, as it can be modeled as a single ray [2].

$$\tilde{y}(t) = h(t)\tilde{x}(t) \quad \text{flat channel.} \quad (2.19)$$

In case of a frequency selective channel the input/output relationship is a convolution given by

$$\tilde{y}(t) = h(\tau, t) * \tilde{x}(t) \quad \text{frequency - selective channel.} \quad (2.20)$$

Two important characteristic quantities that can be derived from the *maximum delay spread* useful for the characterization of frequency selective WSSUS models. The first quantity is known as *average delay* and the second quantity is *delay spread*.

Average delay: The average delay of a frequency selective WSSUS channel is defined by the first moment of $p(\tau)$. It is denoted as $B_{\tau\tau}^{(1)}$ and is given by [1]

$$B_{\tau\tau}^{(1)} = \frac{\int_{-\infty}^{\infty} \tau p(\tau) d\tau}{\int_{-\infty}^{\infty} p(\tau) d\tau} \quad (2.21)$$

The *average delay* gives the statistical mean delay that a signal carrier experiences when it is transmitted over a multipath fading channel.

Delay spread: The delay spread denoted by $B_{\tau\tau}^{(2)}$ is defined as the square root of the second central moment of $p(\tau)$ and is given by [1]

$$B_{\tau\tau}^{(2)} = \sqrt{\frac{\int_{-\infty}^{\infty} (\tau - B_{\tau\tau}^{(1)})^2 p(\tau) d\tau}{\int_{-\infty}^{\infty} p(\tau) d\tau}} \quad (2.22)$$

2.3.2 Spaced-Frequency Correlation Function:

The *spaced-frequency correlation function* also known as *frequency correlation function* denoted as $P(\Delta v)$ is defined as the Fourier transform of the *power delay profile* and is given by

$$\begin{aligned} P(\Delta f) &= F(p(\tau)) \\ &= \int_{-\infty}^{\infty} \int_{-\infty}^{\infty} S(\tau, f) e^{-j2\pi v \tau} d\tau df \\ &= \int_{-\infty}^{\infty} S(\tau) e^{-j2\pi v \tau} d\tau \end{aligned} \quad (2.23)$$

The *frequency correlation function* helps in characterization of signal dispersion in frequency domain. $P(\Delta f)$ gives the correlation between two narrowband signals with two different frequencies v_1 and v_2 as a function of frequency difference denoted as Δv given by $\Delta v = v_2 - v_1$. Figure 2.3 shows an example spaced-frequency correlation function.

Coherence bandwidth: The *coherence bandwidth* denoted by B_c and is defined as the frequency separation where all the frequency component amplitudes are correlated. The coherence bandwidth is inversely proportional to the *delay spread* $B_{\tau\tau}^{(2)}$ [1]. The ratio of signal bandwidth and the *coherence bandwidth* is an important factor which determines the complexity of the signal equalization in the receiver, if the ratio is large then the complexity of the equalization grows and vice versa. A channel can be classified as a frequency selective or frequency nonselective based on the relationship between the *coherence bandwidth* B_c and the signal bandwidth B .

- If the *coherence bandwidth* B_c is less than the signal bandwidth B i.e., if $B_c < B$ then the channel is referred as a frequency selective channel. The channel acts a filter and hence the frequency selective fading occurs.
- The channel is referred as a frequency nonselective if the *coherence bandwidth* is greater than the channel bandwidth i.e., if $B_c > B$, as mentioned before in previous section

frequency nonselective channel does not introduce ISI into the received signal, but the SNR of the received signal decreases.

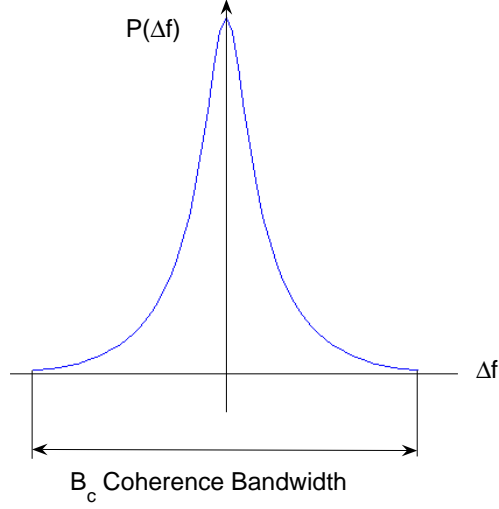


Figure 2.3: The Spaced-Frequency Correlation Function.

2.3.3 Doppler power spectrum:

The mobile radio propagation environment is time-varying because the mobile receiver is in motion and the propagation path changes due to the relative motion between the transmitter and receiver. The relative motion between the transmitter and receiver introduces the frequency spread in the received signal known as the *Doppler spread*. The time varying nature of the channel is characterized (in frequency domain) by *Doppler power spectrum* denoted as $S(f)$. The *Doppler power spectrum* can be either a Gaussian power spectrum or a Jakes

spectrum, in our work assumed it to be Jakes power spectrum, and is given by

$$S(f) = \frac{1}{\pi f_m \sqrt{1 - (\frac{f}{f_m})^2}}, \quad |f| \leq f_m \quad (2.24)$$

where f_m denotes the maximum Doppler frequency given by (1.1). An example Doppler power spectrum is shown in Figure 2.4.

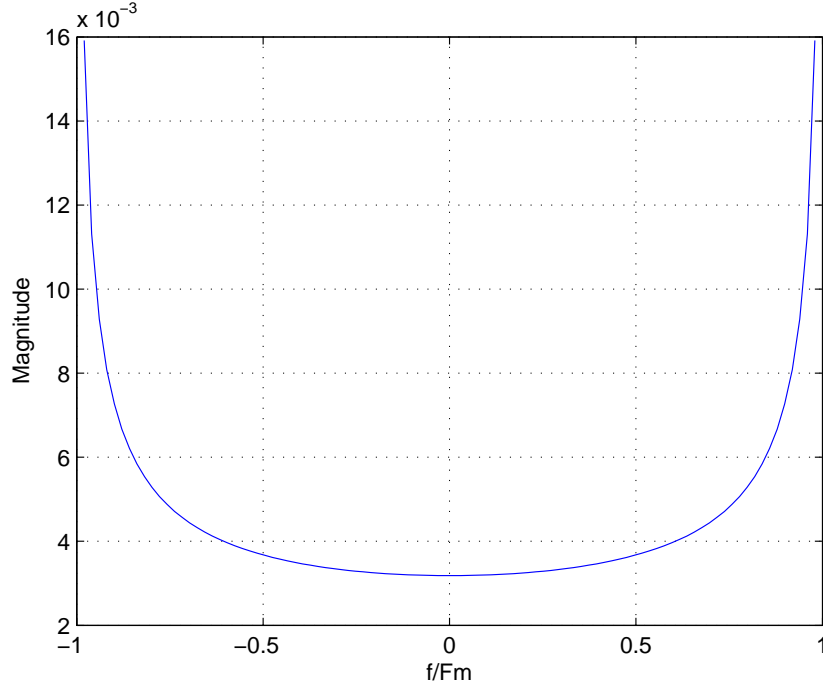


Figure 2.4: Doppler power spectrum.

2.3.4 Spaced-Time Correlation Function:

The *spaced-time correlation function* also known as the *time correlation function*, denoted as $\rho(\tau)$ is obtained by calculating the inverse fourier transform of the Doppler power spectrum given by [2]

$$\rho(\Delta t) = F^{-1}(S(f)) = J_0(2\pi f_m \Delta t), \quad (2.25)$$

where $J_0(\cdot)$ denotes the zeroth-order Bessel function. The *space-time correlation function* gives the amount of correlation between the different scatterers received at times t_1 and t_2

as a function of the time difference Δt given by $\Delta t = t_2 - t_1$. The *coherence time* denoted as T_c is defined as the time interval where the two scattered components remain correlated. A channel can be classified as a *fast fading* or *slow fading* channel based on the relationship between the *coherence time* T_c and the symbol time T_{sym} . Figure 2.4 shows an example of spaced-time correlation function.

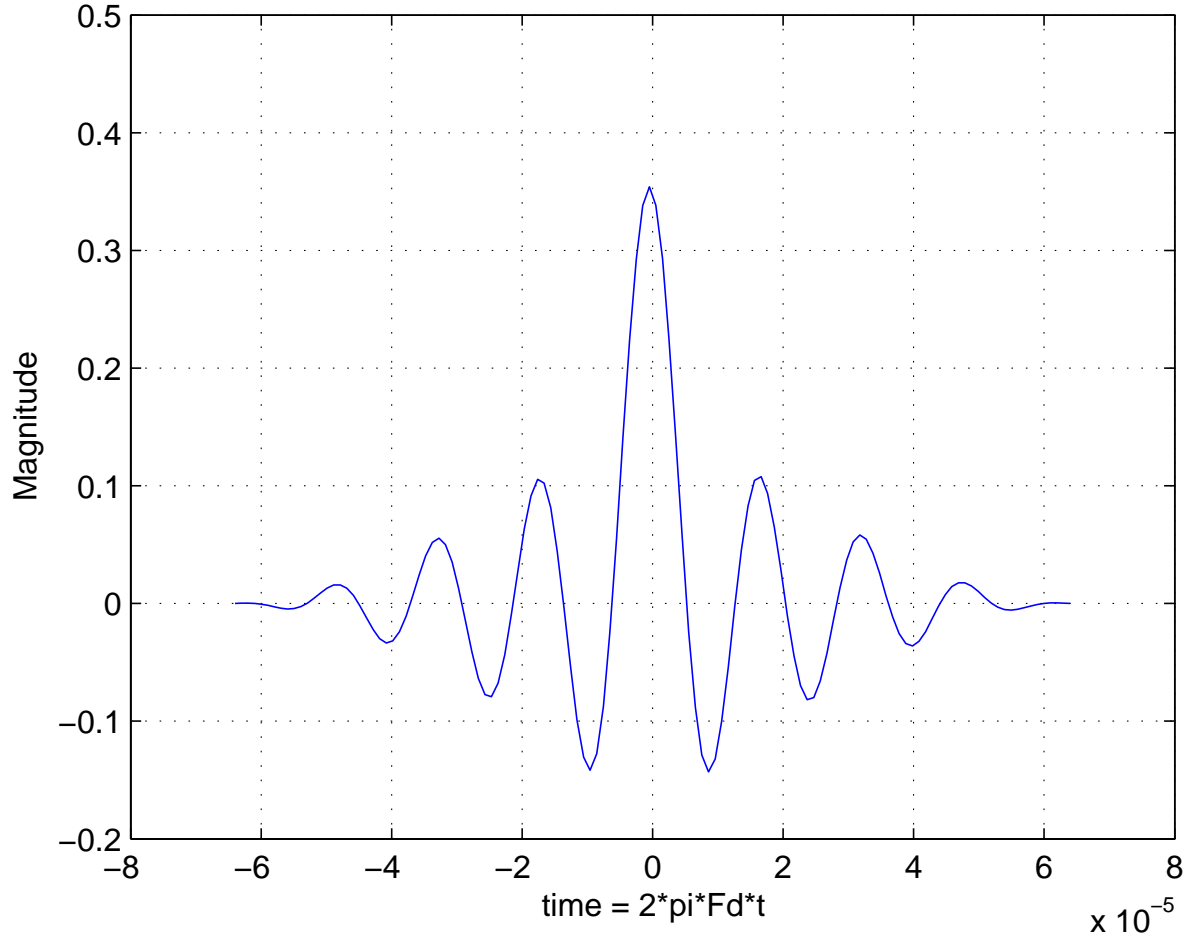


Figure 2.5: The Spaced-Time Correlation Function.

- If the *coherence time* T_c is greater than the symbol time T_{sym} i.e., $T_c > T_{sym}$ then the channel is considered to be a slow fading channel. The channel impulse response can be assumed constant for that symbol time period.

- The channel is considered a *fast fading* channel if the *coherence time* T_c is less than the symbol time T_{sym} i.e., $T_c < T_{sym}$. In a fast fading channel the channel variations are fast when compared to the symbol time period resulting in severe distortion of the signal which effects the signal synchronization and also the BER is high.

The *Doppler power spectrum* yields information about the amount of spectral broadening introduced into the received signal due to relative motion between the transmitter and receiver. The *Doppler power spectrum* is considered as the dual of the $\rho(\tau)$ as the latter yields information about the pulse spreading in the time domain. The *Doppler power spectrum* is helpful in estimating the amount of frequency spread introduced into the signal due to channel time variations. The maximum doppler spread f_m is also called the *fading bandwidth* of the channel. The Doppler power spectrum $S(f)$ and the time correlation function form a Fourier transform pair the Doppler spread f_m and the *coherence time* T_c are inversely proportional and is given by [2]

$$T_c \propto \frac{1}{f_m} \quad (2.26)$$

Chapter 3

Methods for Simulation of Multipath-Fading Channels

3.1 Introduction

To realize any multipath channel model at least two real-valued Gaussian random processes are required. For example, to model a Rayleigh process $\zeta(t)$ given by the absolute value of a zero-mean complex Gaussian random process $\mu(t)$ given by

$$\mu(t) = \mu_1(t) + j\mu_2(t), \quad (3.1)$$

requires realization of two real-valued Gaussian random processes $\mu_1(t)$ and $\mu_2(t)$. Rice process denoted as $\xi(t)$ and is given by

$$\xi(t) = |\mu_p(t)| = |\mu(t) + m(t)|, \quad (3.2)$$

where $\mu(t)$ represents the zero-mean complex Gaussian random process given by (3.1) also requires two real-valued Gaussian random variables. The statistical amplitude behavior of the received signal in the multipath channels can be described by Rayleigh, Rice or Suzuki processes. Based on this statistical amplitude behavior they are denoted as Rayleigh, Rice or Suzuki channels. These channels represent the group of frequency nonselective channels. The frequency selective channel can be modeled as a time-variant finite impulse response (FIR) filter with \mathcal{L} time-variant complex-valued Gaussian coefficients and this requires realization of $2\mathcal{L}$ real-valued colored Gaussian random processes. From the examples, it becomes clear that the development of efficient methods to realize colored Gaussian random processes is very important in the modeling of both frequency selective and frequency nonselective channels.

In this chapter we present few methods to realize colored Gaussian random processes with specified power spectral density and autocorrelation functions.

3.2 Deterministic Channel Modeling

The two fundamental methods widely used for modeling of coloured Gaussian random processes are *filter method* and *rice method*.

3.2.1 Filter Method

The filter method realizes a coloured Gaussian random process by filtering white Gaussian noise (WGN) $v(t)$ through a time-invariant filter $h(t)$, as shown in the Figure 3.1. The frequency response of the filter is matched to the desired power spectral density, in our work it is Jakes power spectral density. Assuming $v(t)$ to be *zero mean, unit variance* white Gaussian noise, at the output we have a *zero mean* coloured Gaussian random process $\mu(t)$. The power spectral density of the $\mu(t)$ matches the square of the absolute value of the filter transfer function $H(f)$ given by [1]

$$S_{\mu\mu}(f) = |H(f)|^2. \quad (3.3)$$

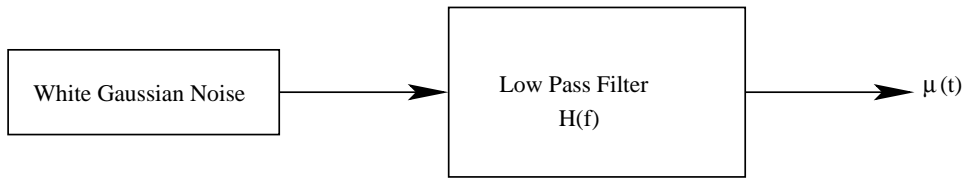


Figure 3.1: Filter method to model a colored Gaussian random process.

The disadvantage of filter method is that it requires higher order filter to approximate the Doppler spectrum and that significantly increases the complexity of the simulator.

3.2.2 Rice Method

The Rice method is based on superposition of an infinite number of weighted sinusoids with equidistant frequencies and random phases as shown in the Figure 3.2. The stochastic Gaussian process generated by the Rice method can be described mathematically as [1]

$$\mu(t) = \lim_{N \rightarrow \infty} \sum_{n=1}^N c_n \cos(2\pi f_n t + \theta_n), \quad (3.4)$$

$$\text{where } c_n = 2\sqrt{(\Delta f S_{\mu\mu}(f_n))} \quad (3.5)$$

$$\text{and } f_n = n \Delta f \quad (3.6)$$

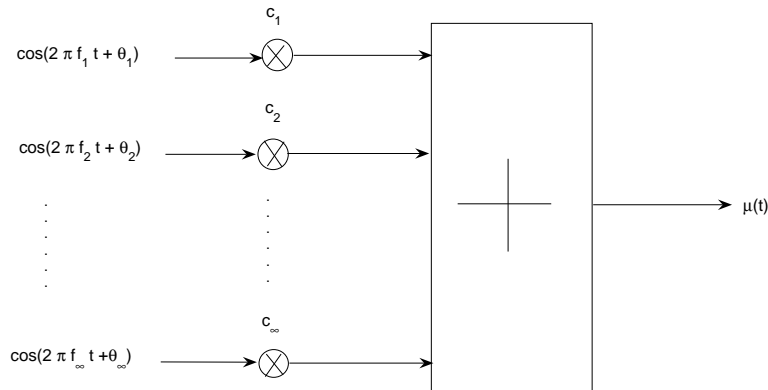


Figure 3.2: Rice method to model a colored Gaussian random process.

The phases denoted by θ_n , where $n = 1, 2, \dots, N$ are random variables with uniform probability density function in the interval $(0, 2\pi]$. In Equation (3.4) the quantity Δf is chosen

such that f_n covers the relevant frequency range, and further care is taken in choosing the value of Δf so that it satisfies the property: $\Delta f \rightarrow 0$ as $N \rightarrow \infty$.

The Rice method generates a zero-mean Gaussian random process with power spectral density $S_{\mu\mu}(f)$. The above two methods generate an identical stochastic process and both the methods are difficult to realize. Using filter method the exact realization is prevented by the fact that it's difficult to attain an ideal response and also the input white Gaussian noise is difficult to realize. Using Rice method the exact realization is prevented by the fact that an infinite number of harmonic functions N is not feasible to implement on a computer or any other hardware platform. The filter method makes it possible to realize a stochastic simulation model by using a non ideal filter which is realizable. The filter output signal statistics deviate from the desired ideal Gaussian random process and it depends on the extent of the realizable expenditure.

The Rice method is implemented by using only a finite number of harmonic functions and the process obtained is denoted by $\hat{\mu}(t)$ and is given by [1]

$$\hat{\mu}(t) = \sum_{n=1}^N c_n \cos(2\pi f_n t + \theta_n), \quad (3.7)$$

where the parameters c_n and f_n are given by Equations (3.5) and (3.6) respectively and the random phase θ_n is uniformly distributed random variable. The random process generated by (3.7) approaches (3.4) as the number of harmonic functions reach infinity i.e., $\hat{\mu}(t) \rightarrow \mu(t)$ as $N \rightarrow \infty$. The phases of the simulation model given by (3.7) are uniformly distributed for all $n = 1, 2, \dots, N$, so the simulation model can be treated as a stochastic process. The phases θ_n become constant quantities once they are generated from the random number generator with uniform distribution in the interval $(0, 2\pi]$, they are now outcomes of a random variable. The process realized by finite number of harmonics using the parameters c_n , f_n , and θ_n which are realizations (outcomes) of a random variable is a *deterministic process* or *deterministic*

function, it is denoted by $\tilde{\mu}(t)$ and is given by [1]

$$\tilde{\mu}(t) = \sum_{n=1}^N c_n \cos(2\pi f_n t + \theta_n). \quad (3.8)$$

The Figure 3.3 depicts the structure of a deterministic simulation model. The deterministic simulation model is derived from a stochastic simulation model and the deterministic process satisfies the property as limit $N \rightarrow \infty$ the deterministic process $\tilde{\mu}(t)$ tends to a sample function of the stochastic process $\mu(t)$. Using the deterministic simulation approach, a very close approximate of the underlying Gaussian random process can be realized. The deterministic process $\tilde{\mu}(t)$ approximates the statistical properties of the Gaussian random process $\mu(t)$. The deterministic process obtained by Equation (3.8) represents a *real deterministic Gaussian process* [1]. A complex deterministic Gaussian random process is obtained by adding two real valued deterministic Gaussian random processes given by

$$\tilde{\mu}(t) = \tilde{\mu}_1(t) + j\tilde{\mu}_2(t) \quad (3.9)$$

where $\tilde{\mu}_1(t)$ and $\tilde{\mu}_2(t)$ denote the real valued Gaussian random processes. The envelope distribution of (3.9) is Rayleigh distributed and it is referred as *deterministic Rayleigh process* given by

$$\tilde{\zeta}(t) = |\tilde{\mu}(t)| = |\tilde{\mu}_1(t) + j\tilde{\mu}_2(t)|. \quad (3.10)$$

If there is a line-of-sight component in the received signal denoted by $m(t)$ the envelope distribution of the process $\tilde{\mu}_p(t) = \tilde{\mu}(t) + m(t)$ is a *deterministic Rice process* [1] given by

$$\tilde{\xi}(t) = |\tilde{\mu}_p(t)| = |\tilde{\mu}(t) + m(t)|. \quad (3.11)$$

The simulation model required for computer simulations is obtained by sampling the continuous time deterministic process. The continuous time variable t is replaced by the variable with $t = kT_s$, where T_s denotes the sampling time interval and k is an integer. The parameters of simulation model c_n , f_n , and θ_n for $n = 1, 2, \dots, N$ need to be determined before carrying out the computer simulations.

The parameters c_n , f_n , and θ_n are kept constant for the entire duration of simulation. The parameters c_n , f_n , and θ_n are called as *Doppler coefficients*, *discrete Doppler frequencies*, and *Doppler phases* respectively as these parameters are used for modeling time-variant multipath channels caused by Doppler effect.

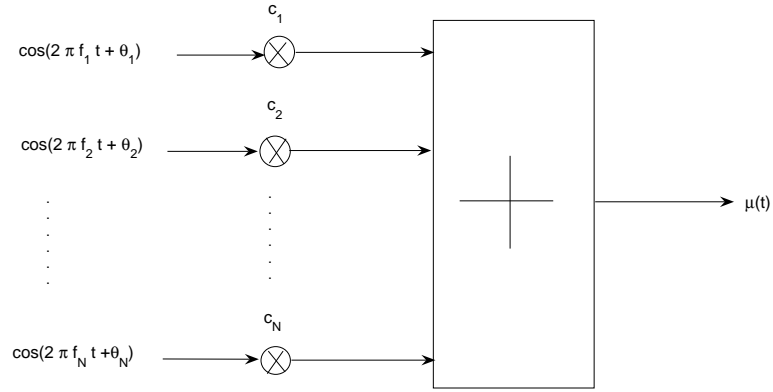


Figure 3.3: Deterministic simulation model for coloured Gaussian random processes [1].

3.3 Properties of Deterministic Processes

In this section we present the fundamental characteristic quantities of deterministic processes like autocorrelation function, power spectral density, etc

Mean value: Consider a deterministic process $\mu(t)$ with $f_n \neq 0$ holds for all values of n .

The mean value of $\tilde{\mu}(t)$ denoted as \tilde{m}_μ is given by

$$\begin{aligned}\tilde{m}_\mu &= \lim_{T \rightarrow \infty} \frac{1}{2T} \int_{-T}^T \tilde{\mu}(t) dt \\ &= 0\end{aligned}\tag{3.12}$$

Mean power: The mean power of a deterministic process $\tilde{\mu}(t)$ is defined as

$$\tilde{\sigma}_\mu^2 = \lim_{T \rightarrow \infty} \frac{1}{2T} \int_{-T}^T |\tilde{\mu}(t)|^2 dt,\tag{3.13}$$

substituting (3.8) in the above equation, mean power of the deterministic process is given by

$$\tilde{\sigma}_\mu^2 = \sum_{n=1}^N \frac{c_n^2}{2}.\tag{3.14}$$

Autocorrelation function: The autocorrelation function of a deterministic process $\tilde{\mu}(t)$ denoted as $\tilde{r}_{\mu\mu}(\tau)$ is defined as

$$\tilde{r}_{\mu\mu}(\tau) = \lim_{T \rightarrow \infty} \frac{1}{2T} \int_{-T}^T \tilde{\mu}^*(t) \tilde{\mu}(t + \tau) dt,\tag{3.15}$$

from (3.15) the autocorrelation function of the deterministic process $\tilde{\mu}(t)$ is

$$\tilde{r}_{\mu\mu}(\tau) = \sum_{n=1}^N \frac{c_n^2}{2} \cos(2\pi f_n \tau).\tag{3.16}$$

By observing the above equation closely one can notice that the autocorrelation function depends on the Doppler coefficients c_n and the discrete Doppler frequencies f_n . By comparing equations (3.14) and (3.16) it is clear that the mean power of the deterministic process is the value of autocorrelation function at the point $\tau = 0$ i.e., $\tilde{\sigma}_\mu^2 = \tilde{r}_{\mu\mu}(0)$.

Cross-correlation function: Consider two deterministic random processes $\tilde{\mu}_1(t)$ and $\tilde{\mu}_2(t)$ the cross correlation function $\tilde{r}_{\mu_1\mu_2}(\tau)$ is defined as

$$\tilde{r}_{\mu_1\mu_2}(\tau) = \lim_{T \rightarrow \infty} \frac{1}{2T} \int_{-T}^T \tilde{\mu}_1^*(t) \tilde{\mu}_2(t + \tau) dt,\tag{3.17}$$

from the above equation the cross-correlation function of $\tilde{\mu}_1(t)$ and $\tilde{\mu}_2(t)$ is

$$\tilde{r}_{\mu_1\mu_2}(\tau) = 0, \quad \text{if } f_{1,n} \neq \pm f_{2,m}, \quad (3.18)$$

the above equation holds for all $n = 1, 2, \dots, N_1$ and $m = 1, 2, \dots, N_2$. Equation(3.18) shows that if absolute values of the Doppler frequencies of the respective deterministic processes $\tilde{\mu}_1(t)$ and $\tilde{\mu}_2(t)$ are different, then the deterministic processes are uncorrelated. If $f_{1,n} = f_{2,m}$ for all or some pairs of (n, m) then the deterministic processes are correlated and the cross-correlation function is given by [1]

$$\tilde{r}_{\mu_1\mu_2}(\tau) = \sum_{n=1}^N \frac{c_{1,n}c_{2,m}}{2} \cos(2\pi f_{1,n}\tau - \theta_{1,n} \pm \theta_{2,m}), \quad (3.19)$$

where N takes the value of the largest number of N_1 and N_2 i.e., $N = \max\{N_1, N_2\}$. The equation (3.19) shows that the cross-correlation function $\tilde{r}_{\mu_1\mu_2}(\tau)$ depends on the Doppler phases $\theta_{i,n}$ where $i = 1, 2$. The cross-correlation function of the deterministic processes $\tilde{\mu}_2(t)$ and $\tilde{\mu}_1(t)$ denoted as $\tilde{r}_{\mu_2\mu_1}(\tau)$ is obtained from the relation

$$\tilde{r}_{\mu_2\mu_1}(\tau) = \tilde{r}_{\mu_1\mu_2}^*(-\tau) = \tilde{r}_{\mu_1\mu_2}(-\tau)$$

Power spectral density: The power spectral density $\tilde{S}_{\mu\mu}(f)$ of a deterministic process $\tilde{\mu}(t)$ is obtained by applying Fourier transform to the autocorrelation function (3.17) and is given by

$$\tilde{S}_{\mu\mu}(f) = \int_{-\infty}^{\infty} \tilde{r}_{\mu\mu}(\tau) e^{-j2\pi f\tau} d\tau, \quad (3.20)$$

from above equation, the power spectral density of the deterministic process $\tilde{\mu}(t)$ is given by

$$\tilde{S}_{\mu\mu}(f) = \sum_{n=1}^N \frac{c_n^2}{4} [\delta(f - f_n) + \delta(f + f_n)]. \quad (3.21)$$

The power spectral density given by (3.21) is a symmetrical function i.e., $\tilde{S}_{\mu\mu}(f) = \tilde{S}_{\mu\mu}(-f)$.

Periodicity: Consider a deterministic process $\tilde{\mu}(t)$ with nonzero arbitrary parameters c_n , f_n , and θ_n . If the discrete Doppler frequencies f_n have a greatest common divisor denoted as F and given by

$$F = \gcd\{f_1, f_2, \dots, f_N\} \quad (3.22)$$

then the deterministic process $\tilde{\mu}(t)$ is periodic with time period T given by $T = 1/F$ and $\tilde{\mu}(t) = \tilde{\mu}(t + T)$ and the autocorrelation function $\tilde{r}_{\mu\mu}(\tau + T) = \tilde{r}_{\mu\mu}(\tau)$.

3.4 Methods to Compute the Model Parameters for Deterministic Processes

As mentioned in the previous section, to realize a simulation model for the computer simulations, the first step is to determine the parameters of the simulation model c_n , f_n , and θ_n for $n = 1, 2, \dots, N$. There are multitude of methods specified in [1] to generate the *Doppler coefficients*, *Doppler frequencies*, *Doppler phases*, we consider the *method of equal areas* (MEA) and *method of exact Doppler spread* (MEDS), to calculate the simulation model parameters. The above mentioned methods are used in calculating the *Doppler coefficients*, *Doppler frequencies* and the *Doppler phases* θ_n can be computed independently irrespective of the method used to calculate the Doppler coefficients and Doppler frequencies.

As mentioned before in the previous section as the number of harmonic functions reach infinity i.e., as $N \rightarrow \infty$ the statistical properties of the simulation model match the reference model exactly. This property also implies to the various methods used to generate the parameters of the simulation model and all the methods generate the deterministic process whose statistical properties are identical and match the reference model exactly. Using finite number of harmonic functions the statistics of the deterministic processes deviate largely from their reference models. The above said methods are applied to Jakes power spectral density to obtain simple equations to calculate the desired model parameters for practical applications.

3.4.1 Method of Equal Areas (MEAS)

The method of equal areas calculates the discrete doppler frequencies in such a way that the area of Doppler spectral density $S_{\mu\mu}(f)$ within the frequency range $f_{n-1} < f \leq f_n$ is equal to $\sigma_0^2/(2N)$ i.e.,

$$\int_{f_{n-1}}^{f_n} S_{\mu\mu}(f) df = \frac{\sigma_0^2}{2N}, \quad (3.23)$$

for all $n = 1, 2, \dots, N$ and the value of $f_0 = 0$. To calculate the values of the discrete Doppler frequencies an auxiliary function is introduced which is defined as [1]

$$G_\mu(f_n) = \int_{-\infty}^{f_n} S_{\mu\mu}(f) df. \quad (3.24)$$

If the Doppler spectrum is symmetrical i.e., $S_{\mu\mu}(f) = S_{\mu\mu}(-f)$ then using Equation (3.23) the auxiliary function (3.24) is expressed in the form [1]

$$\begin{aligned} G_\mu(f_n) &= \frac{\sigma_0^2}{2} + \sum_{k=1}^n \int_{f_{k-1}}^{f_k} S_{\mu\mu}(f) df \\ &= \frac{\sigma_0^2}{2} \left(1 + \frac{n}{N}\right). \end{aligned} \quad (3.25)$$

The discrete Doppler frequencies are calculated by taking the inverse of the function G_μ , which is denoted as G_μ^{-1} and the discrete Doppler frequencies are given by [1]

$$f_n = G_\mu^{-1} \left[\frac{\sigma_0^2}{2} \left(1 + \frac{n}{N}\right) \right], \quad (3.26)$$

for all $n = 1, 2, \dots, N$. The discrete Doppler coefficients are determined by imposing a condition which states that the mean power of the stochastic process $\mu(t)$ is identical to that of the deterministic process $\tilde{\mu}(t)$ within the frequency interval $I_n = (f_{n-1}, f_n]$ i.e.,

$$\int_{f \in I_n} S_{\mu\mu}(f) df = \int_{f \in I_n} \tilde{S}_{\mu\mu}(f) df. \quad (3.27)$$

The Doppler coefficients are given by

$$c_n = \sigma_0 \sqrt{\frac{2}{N}}, \quad (3.28)$$

for all $n = 1, 2, \dots, N$. Applying the above procedure to the Jakes power spectral density we get the discrete Doppler coefficients and Doppler frequencies.

Jakes power spectral density: Using the Jakes power spectral density given by (2.22) the expression for auxiliary function is given by [1]

$$G_\mu = \frac{\sigma_0^2}{2} \left[1 + \frac{2}{\pi} \arcsin\left(\frac{f_n}{f_m}\right) \right], \quad (3.29)$$

where f_n satisfies the condition $0 < f_n < f_m$, for all $n = 1, 2, \dots, N$. The discrete doppler coefficients are calculated by substituting the value of the auxiliary function given by (3.25) into (3.29) and are given by

$$f_n = f_m \sin\left(\frac{\pi n}{2N}\right) \quad (3.30)$$

This equation is valid for all values of $n = 1, 2, \dots, N$. The discrete Doppler coefficients are given by (3.17). The deterministic process $\tilde{\mu}(t)$ generated by method of equal areas is nonperiodic, this results from the fact that the greatest common divisor F given by $F = \gcd\{f_n\}_{n=1}^N$ is zero. So the time period of the deterministic Gaussian process defined as $T = 1/F$ is infinite. For complex deterministic process $\tilde{\mu}(t) = \tilde{\mu}_1(t) + j\tilde{\mu}_2(t)$ the condition that the real and imaginary parts have to be uncorrelated is satisfied by taking the number of harmonic functions N_2 defined as $N_2 = N_1 + 1$. For any chosen values of N_1 and N_2 the fact that $f_{1,N_1} = f_{2,N_2} = f_m$ (f_m denotes the maximum Doppler frequency) holds, this leads to consequence that real deterministic process $\mu_1(t)$ and $\mu_2(t)$ are not completely uncorrelated, but the resulting correlation between the two processes is small even for moderate values of N_1 and N_2 and thus the effect can be ignored. The Figure 3.4 shows an example power spectral density function $\tilde{S}_{\mu\mu}$ given by (3.21) for $N = 14$ and the Figure 3.5 depicts an autocorrelation function given by (3.16) for $N = 14$. The Doppler coefficients c_n and Doppler frequencies f_n are calculated using Equations (3.28) and (3.30).

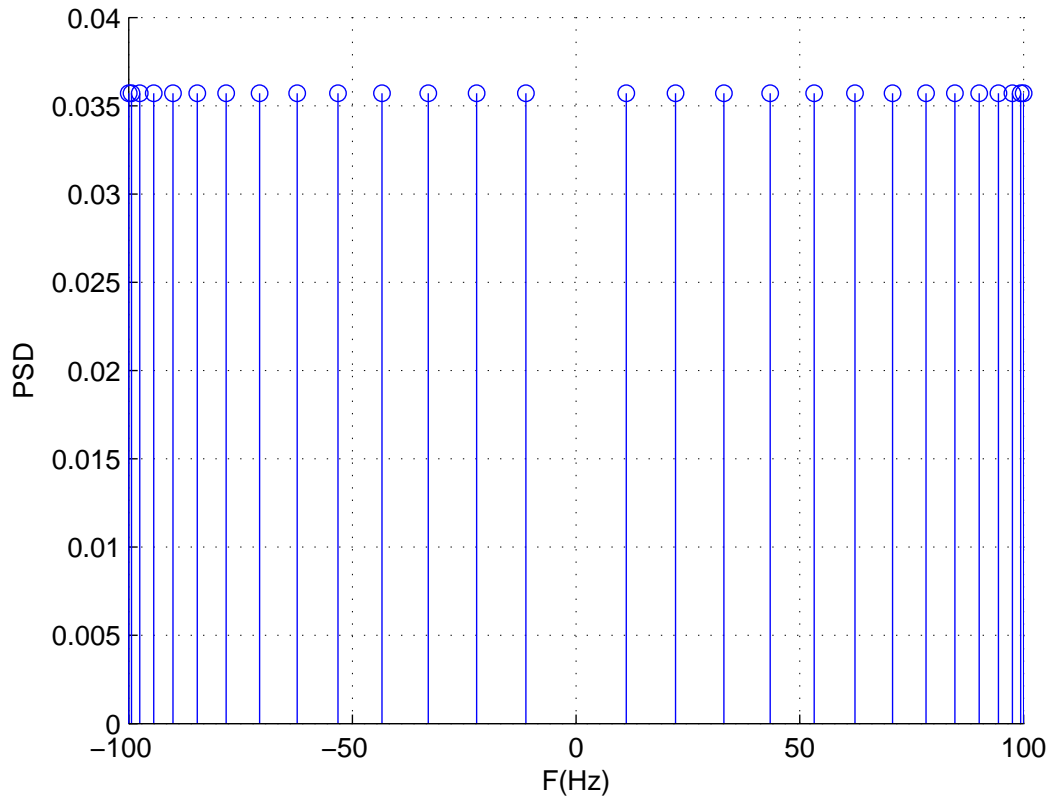


Figure 3.4: Power spectral density $\tilde{S}_{\mu\mu}(f)$ for $N = 14$, $f_m = 100$, $\sigma_0^2 = 1$ (MEAS, Jakes psd).

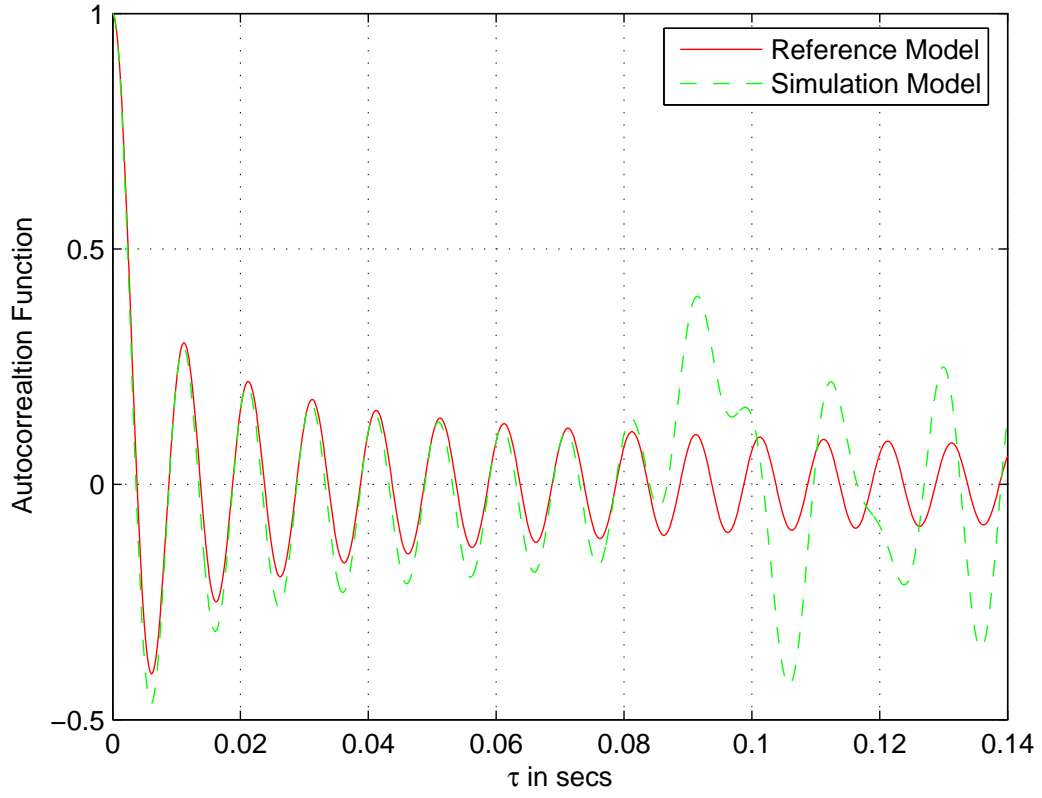


Figure 3.5: Autocorrelation function $\tilde{r}_{\mu\mu}(\tau)$ for $N = 14$, $f_m = 100$, $\sigma_0^2 = 1$ (MEAS, Autocorrelation function).

3.4.2 Method of Exact Doppler Spread (MEDS)

The method of exact Doppler spread (MEDS) was developed for the most widely used Jakes power spectral density. It is a simple method and its performance level when compared to other methods used to calculate model parameters is high. This method enables a very good approximation of the autocorrelation function corresponding to the Jakes power spectral density.

Jakes power spectral density: The first step in deriving the method of exact Doppler spread for calculating the model parameters of Jakes power spectral density starts with an integral representation of zeroth order Bessel function given by

$$J_0(z) = \frac{\pi}{2} \int_0^\pi 2 \cos(z \sin \alpha) d\alpha. \quad (3.31)$$

The above equation in the form of finite series is expressed as [1]

$$J_0(z) = \lim_{N \rightarrow \infty} \frac{2}{\pi} \sum_{n=1}^N \cos(z \sin \alpha_n) \Delta\alpha, \quad (3.32)$$

where the value of $\alpha_n = \pi(\frac{2n-1}{4N})$ and the value of $\Delta\alpha = \pi/(2N)$. The autocorrelation function of the Jakes power spectral density obtained by taking the inverse Fourier transform of $S_{\mu\mu}(f)$ is denoted as $r_{\mu\mu}(\tau)$ and is given by

$$r_{\mu\mu}(\tau) = \sigma_0^2 J_0(2\pi f_m \tau), \quad (3.33)$$

where $J_0(\cdot)$ as said above represents zeroth order Bessel function of first kind and by substituting the values of α_n and $\Delta\alpha$ in (3.32) and by comparing it with the Equation (3.33) the expression for autocorrelation function can be written as

$$r_{\mu\mu}(\tau) = \lim_{N \rightarrow \infty} \frac{\sigma_0^2}{N} \sum_{n=1}^N \cos\{2\pi f_m \sin[\frac{\pi}{2N}(n - \frac{1}{2})] \cdot \tau\}. \quad (3.34)$$

The above relation represents the autocorrelation function for the stochastic reference model of a Gaussian random process $\mu(t)$. To get a relation for the autocorrelation function of the

simulation model from reference model, the limit $N \rightarrow \infty$ is removed from (3.23) and the relation for the autocorrelation function of simulation model denoted as $\tilde{r}_{\mu\mu}(\tau)$ is given by

$$\tilde{r}_{\mu\mu}(\tau) = \frac{\sigma_0^2}{N} \sum_{n=1}^N \cos\{2\pi f_m \sin[\frac{\pi}{2N}(n - \frac{1}{2})] \cdot \tau\}. \quad (3.35)$$

The Doppler coefficients c_n and Doppler frequency coefficients f_n can be obtained by comparing (3.35) with (3.16) and they are given by

$$c_n = \sigma_0 \sqrt{\frac{2}{N}}, \quad (3.36)$$

and

$$f_n = f_m \sin[\frac{\pi}{2N}(n - \frac{1}{2})], \quad (3.37)$$

respectively, for all values of n . The time period of the deterministic process which is given by the greatest common divisor $F = \gcd\{f_n\}_{n=1}^N$ is equal to zero and so the time period T given by $T = 1/F$ becomes infinity. The condition that the two real valued deterministic processes $\tilde{\mu}_1(t)$ and $\tilde{\mu}_2(t)$ in a complex deterministic process should be uncorrelated is satisfied by the taking $N_2 = N_1 + 1$, where N_2 is the number of harmonics for the process $\tilde{\mu}_2(t)$ and N_1 for $\tilde{\mu}_1(t)$. An example power spectral density $\tilde{S}_{\mu\mu}(f)$ and autocorrelation function $\tilde{r}_{\mu\mu}(\tau)$ given by (3.21) and (3.35) are depicted in Figures 3.6 and 3.7 for $N = 14$ and $f_m = 100Hz$. The Doppler coefficients c_n are calculated using (3.36) and the Doppler frequencies are calculated using (3.37).

An autocorrelation function $\tilde{r}_{\mu\mu}(\tau)$ calculated using (3.35) is presented in Figure 3.8 for $N = 25$ and $f_m = 100Hz$. When the two Figures 3.7 and 3.8 are compared, the autocorrelation function $\tilde{r}_{\mu\mu}(\tau)$ shown in Figure (3.8) gives a much better approximation of the autocorrelation function then the one shown in Figure 3.7. The better approximation resulted in Figure 3.8 is due to the fact that as $N \rightarrow \infty$ the $\tilde{\mu}(t) \rightarrow \mu(t)$, where $\tilde{\mu}(t)$ is the simulation model and $\mu(t)$ is the stochastic reference model.

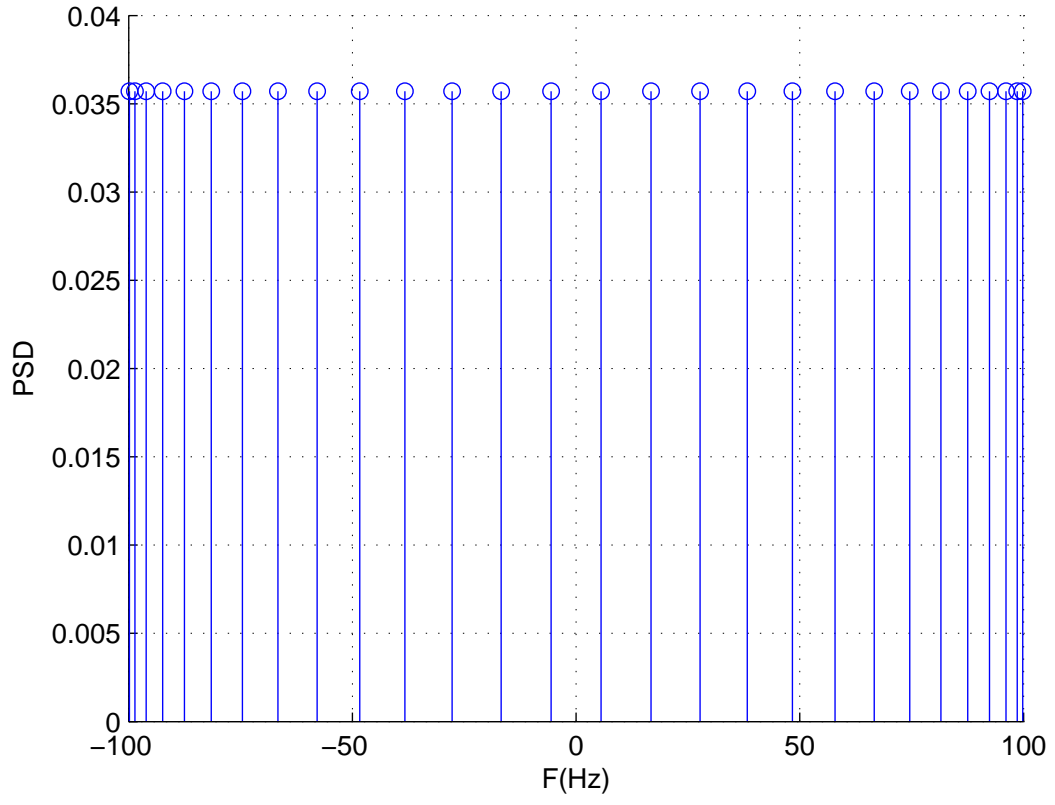


Figure 3.6: Power spectral density $\tilde{S}_{\mu\mu}(f)$ for $N = 14$, $f_m = 100$, $\sigma_0^2 = 1$ (MEDS, Jakes psd).

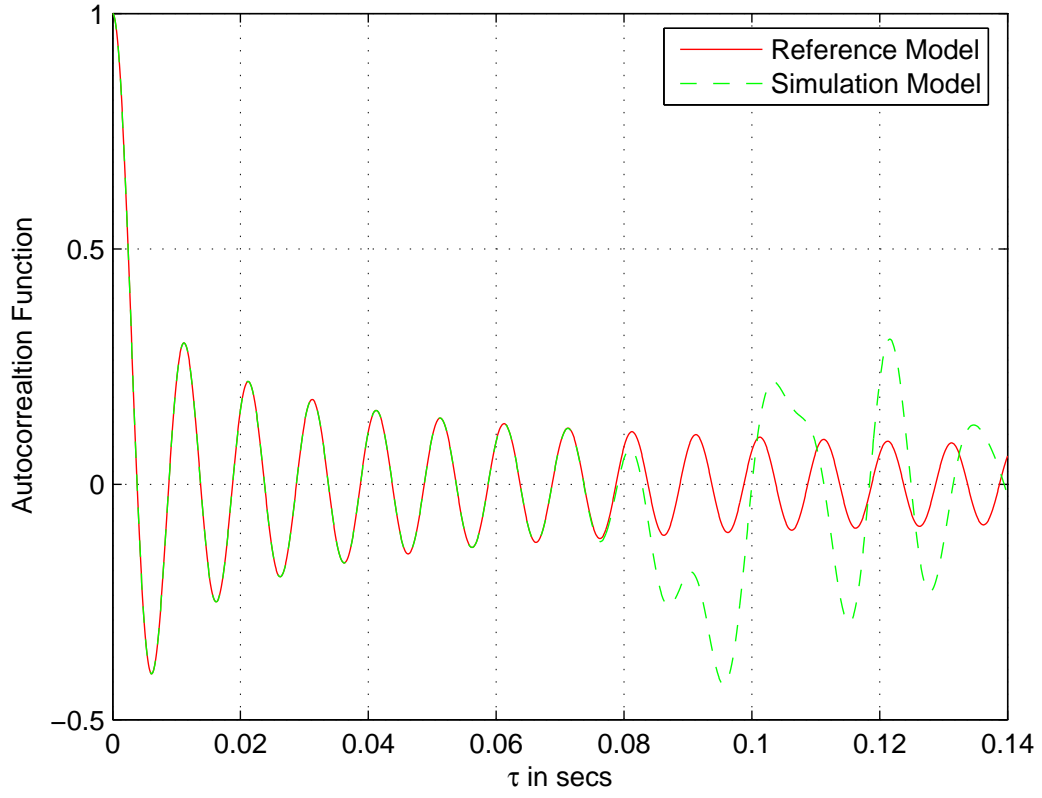


Figure 3.7: Autocorrelation function $\tilde{r}_{\mu\mu}(\tau)$ for $N = 14$, $f_m = 100$, $\sigma_0^2 = 1$ (MEDS, Autocorrelation function).

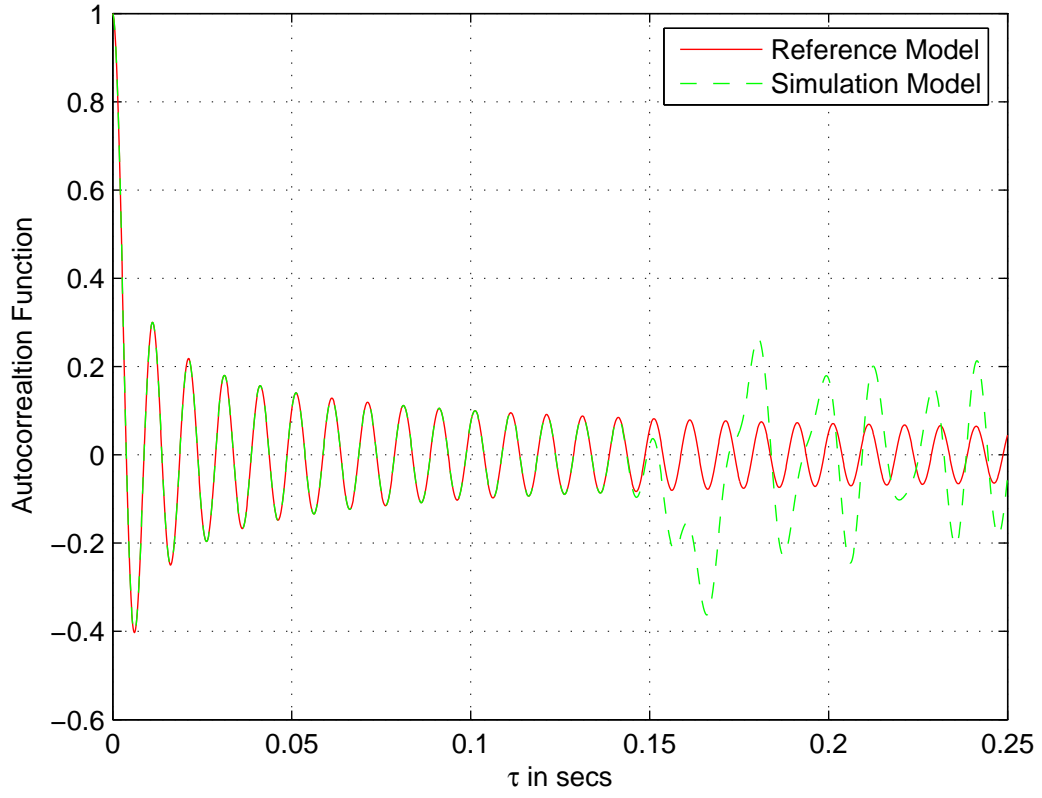


Figure 3.8: Autocorrelation function $\tilde{r}_{\mu\mu}(\tau)$ for $N = 25$, $f_m = 100$, $\sigma_0^2 = 1$ (MEDS, Autocorrelation function).

3.4.3 Doppler Phase Coefficients

The Doppler phase coefficients θ_n are outcomes of a random variable uniformly distributed over the interval $(0, 2\pi]$. Consider a deterministic Rayleigh process $\tilde{\zeta}(t)$ given by (3.10). The underlying deterministic Gaussian processes $\tilde{\mu}_1(t)$ and $\tilde{\mu}_2(t)$ simulation parameters i.e., Doppler coefficients $\{c_{1,n}\}_{n=1}^{N_1}$ and $\{c_{2,n}\}_{n=1}^{N_2}$, and the Doppler frequencies $\{f_{1,n}\}_{n=1}^{N_2}$ and $\{f_{1,n}\}_{n=1}^{N_2}$ were calculated using method of exact Doppler spread. The Doppler phase coefficients $\{\theta_{1,n}\}_{n=1}^{N_1}$ and $\{\theta_{1,n}\}_{n=1}^{N_2}$ are the outcomes of a random variable uniformly distributed over the interval $(0, 2\pi]$. The Figure 3.9 depicts the behavior of $\tilde{\zeta}(t)$ for $N_1 = 25$, and $N_2 = 26$, and the maximum Doppler frequency $f_m = 100$, and $\sigma_0^2 = 1$. The cross-correlation function $\tilde{r}_{\mu_1\mu_2}(t)$ of the two real valued deterministic processes $\tilde{\mu}_1(t)$ and $\tilde{\mu}_2(t)$ in a complex deterministic process depends on the random phases θ_n . In a complex deterministic process if the underlying process $\tilde{\mu}_1(t)$ and $\tilde{\mu}_2(t)$ are uncorrelated then the random Doppler phases do not effect the statistics of the complex deterministic process. From the above discussion it can be concluded that, if the underlying deterministic process in a complex deterministic process are uncorrelated, then the statistics of the signal are independent of random phases θ_n , this conclusion prompts us to set the Doppler phases θ_n equal to zero. By doing so the value of $\tilde{\mu}(0)$ becomes $\sigma_0\sqrt{2N_i}$ ($i = 1, 2$) and the deterministic Rayleigh process $\tilde{\zeta}(t)$ has a maximum value $\sigma_0\sqrt{N_1 + 1/2}$ at the time-instant $t = 0$. This leads to a transient behavior at the origin as shown in Figure 3.10.

Another deterministic method used to calculate Doppler phases θ_n is to generate a standard phase vector denoted as $\vec{\Theta}$ given by [1]

$$\vec{\Theta} = (2\pi \frac{1}{N+1}, 2\pi \frac{2}{N+1}, \dots, 2\pi \frac{N}{N+1}). \quad (3.38)$$

The Doppler phases θ_n are components of the Doppler phase vector given by

$$\vec{\theta} = (\theta_1, \theta_2, \dots, \theta_N), \quad (3.39)$$

the components of the Doppler phase vector $\vec{\theta}$ are the permuted values of the standard

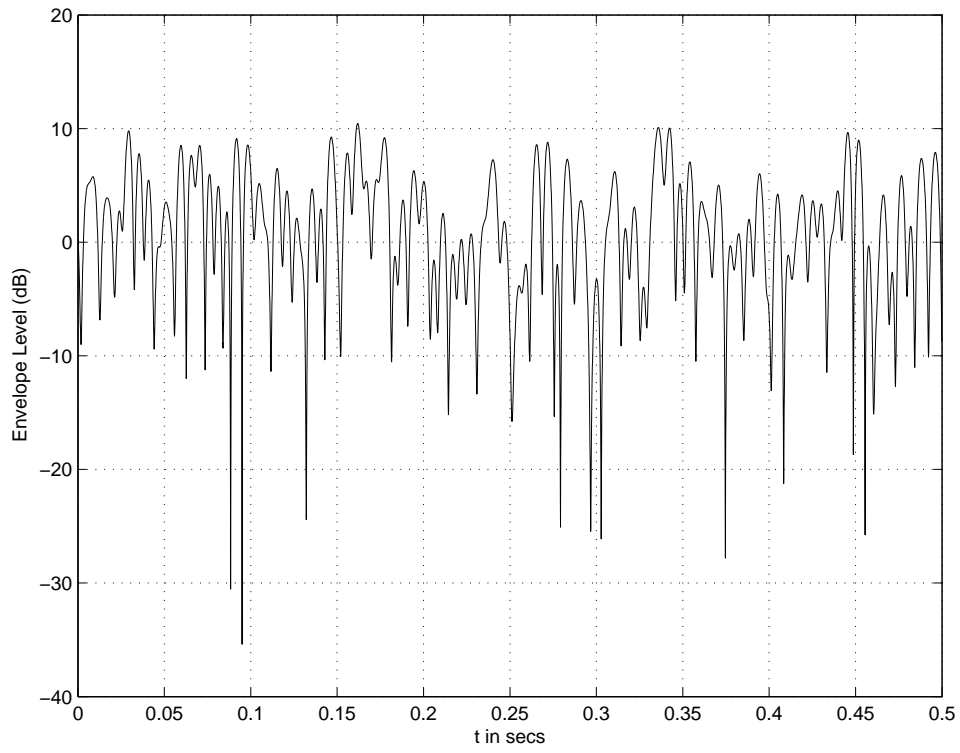


Figure 3.9: Influence of $\theta_{i,n}$ on the behavior of $\tilde{\zeta}(t)$: $\theta_{i,n} \in (0, 2\pi]$.

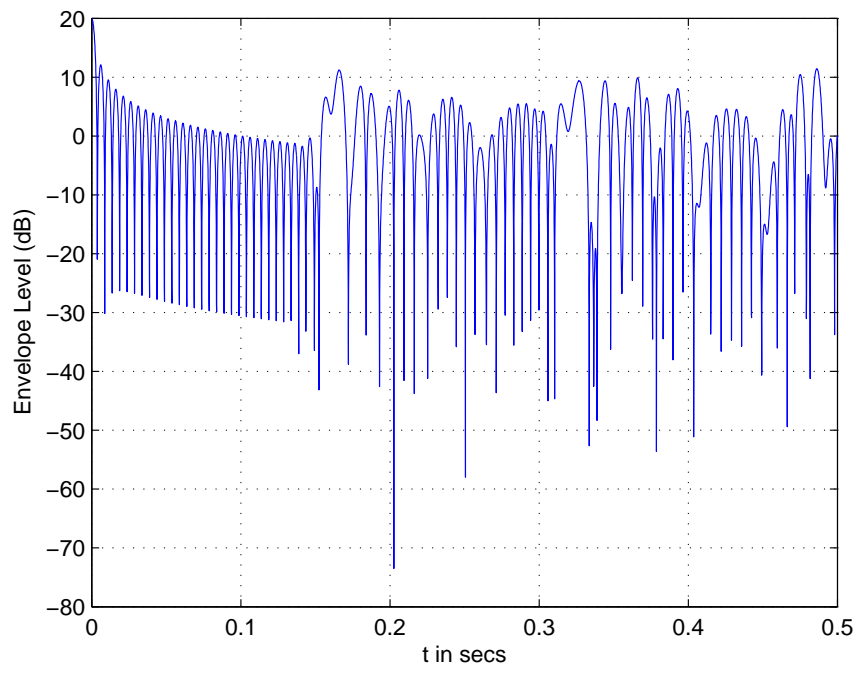


Figure 3.10: Influence of $\theta_{i,n}$ on the behavior of $\tilde{\zeta}(t)$: $\theta_{i,n} = 0$.

phase vector given by (3.38). The resulting deterministic Rayleigh process behavior is as shown in the Figure 3.11.

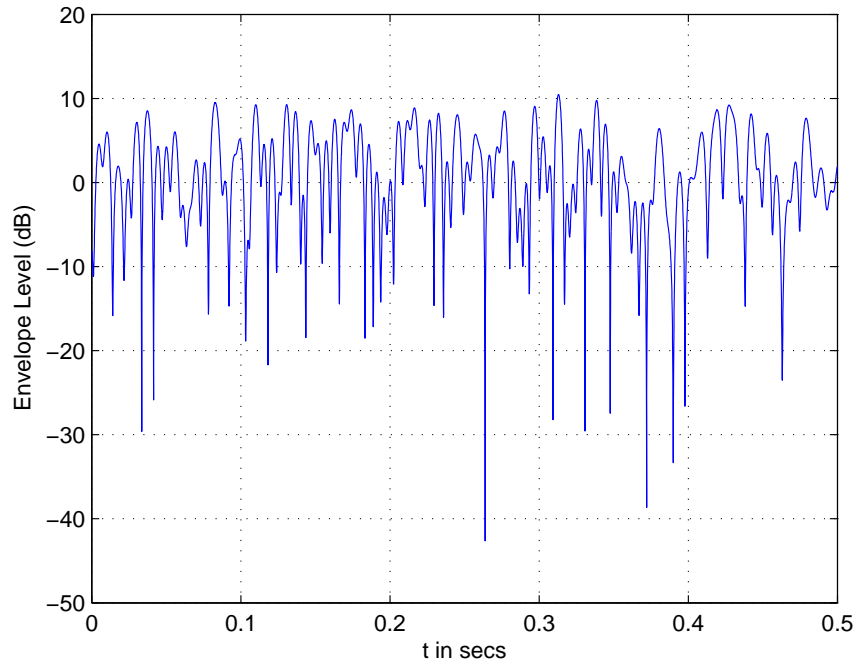


Figure 3.11: Influence of $\theta_{i,n}$ on the behavior of $\tilde{\zeta}(t)$: Permuted phases.

By performing the permutation of the components given by (3.38) it is possible to generate $N!$ different sets of Doppler phases $\{\theta_n\}$.

Chapter 4

Frequency Selective Channel Models

In frequency-nonselective channels the duration of a digitally modulated symbol is greater than the time spread of the multipath propagation path delays. Due to this all the frequencies in the transmitted signal experience same level of random attenuation and phase shift due to multipath fading. The frequency-nonselective channel introduces very little distortion into the received signal. If the propagation path delay differences are large compared to the inverse of the signal bandwidth, then the transmitted signal frequency components will experience different random attenuations and phase shifts along different paths. Due to this the channel introduces amplitude and phase distortions into the transmitted signal and the channel is said to exhibit frequency-selective fading.

To describe the path geometry for a multipath fading channel, Parsons and Bajwa introduced the ellipses model, which is shown in the Figure 4.1 [16]. All ellipses have common focal points, the transmitter and receiver are located at the foci. The different confocal ellipses represent the different delays. The path lengths of the different propagation paths in an ellipse are equal. The Doppler frequencies of the propagation paths with equal path lengths will be different, this is due to the fact that they have different angles of arrival. Referring to the Figure 4.1 the propagation paths (P_2, P_3) and (P_1, P_4) have same path lengths but different Doppler frequencies. The propagation paths with different path lengths will have same Doppler frequencies if the angles of arrival are equal i.e., the propagation paths (P_4, P_3) have different path lengths but same Doppler frequency. The propagation delay associated with each path is determined by its path length and it also depends on the average power of the signal at the receiver antenna.

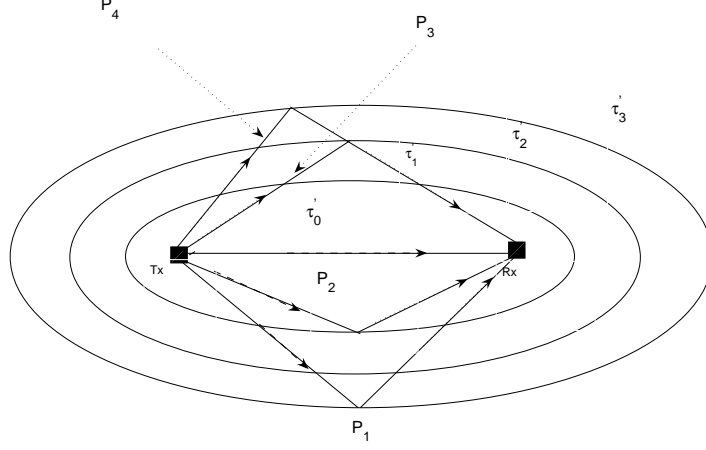


Figure 4.1: Bajwa and Parsons Ellipses Model to describe the multipath signal path geometry [1], [16].

The propagation delays of the different propagation paths in an ellipse are equal. This is due to that fact that the propagation delay is determined by the path length and in an ellipse all the propagation paths have equal length. The *discrete propagation delay* associated with the ℓ th ellipse is given by [1]

$$\tau'_\ell = \tau'_0 + \ell \Delta\tau', \quad \ell = 0, 1, \dots, \mathcal{L} - 1, \quad (4.1)$$

where τ'_0 is the propagation delay of the line-of-sight component, \mathcal{L} gives the total number of paths with different propagation delays, and $\Delta\tau'$ is an infinitesimal propagation delay. As the number of paths \mathcal{L} with different propagation delays increase the $\Delta\tau'$ becomes smaller and the precision of ellipses model increases. As the limit $\mathcal{L} \rightarrow \infty$ the infinitesimal propagation delay $\Delta\tau' \rightarrow 0$ and the discrete propagation delay τ'_ℓ becomes a *continuous propagation delay* τ' . The continuous propagation delay τ' is restricted to the interval $[\tau'_0, \tau'_m]$, where τ'_m

represents the maximum propagation delay and all the scattered components having propagation delays τ' greater than τ'_m are ignored.

4.1 COST 207 Channel Models

In this section we present the channel models according to COST 207. The COST 207 models were developed and standardized for GSM Systems. The propagation environments defined in the COST 207 study, are classified into four typical areas known as Rural Area (RA) for areas with rural characteristics, Bad Urban (BU) propagation environment for the densely built urban areas, Typical Urban (TU) propagation environment for cities and suburbs, and Hilly Terrain (HT) for hilly regions. The COST 207 models specified Doppler power spectral density and the delay power spectral density for these four propagation environments. The delay power spectral densities $S_{\tau'\tau'}(\tau')$ specified for the typical propagation environments are given below.

Rural Area (RA):

$$\begin{aligned} S_{\tau'\tau'}(\tau') &= C_{RA}e^{-9.2\tau'/\mu s}, & 0 \leq \tau' \leq 0.7\mu s \\ &= 0, & else, \end{aligned} \quad (4.2)$$

where C_{RA} is a real valued constant coefficient given by

$$C_{RA} = \frac{9.2}{1 - e^{-6.44}}, \quad (4.3)$$

the delay spread $B_{\tau'\tau'}^{(2)} = 0.1\mu s$, which is defined as the square root of the second central moment of $S_{\tau'\tau'}(\tau')$ and given by (2.20). Figure 4.2 depicts the typical rural area power delay profile.

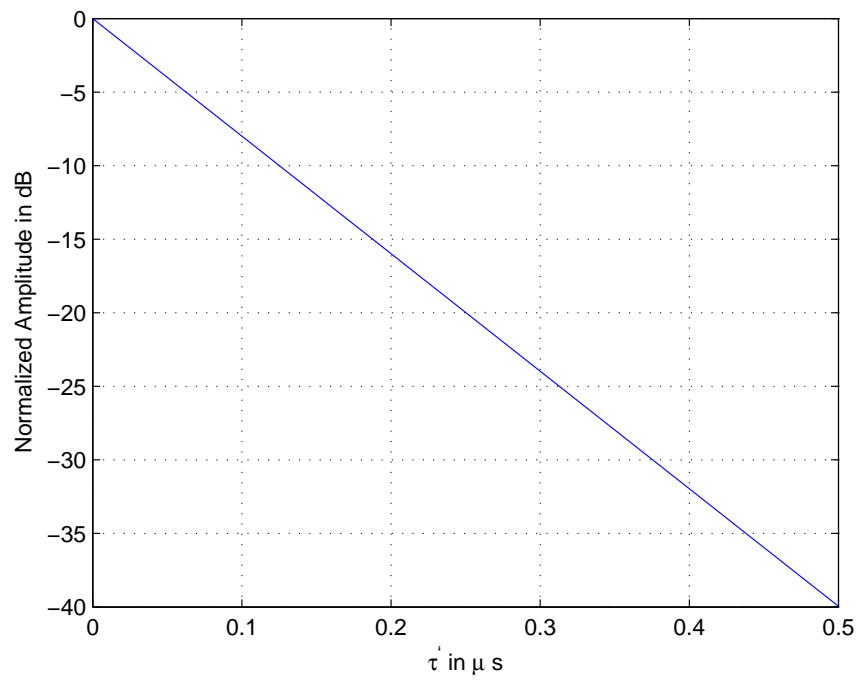


Figure 4.2: Delay power spectral density $S_{\tau'\tau'}(\tau')$ for Rural Area (RA).

Typical Urban (TU):

$$\begin{aligned} S_{\tau'\tau'}(\tau') &= C_{TU}e^{-\tau'/\mu s}, & 0 \leq \tau' \leq 7\mu s \\ &= 0, & else, \end{aligned} \quad (4.4)$$

where the real valued coefficient C_{TU} is given by

$$C_{TU} = \frac{1}{1 - e^{-7}} , \quad (4.5)$$

the delay spread for the Typical Urban channel model $B_{\tau'\tau'}^{(2)} = 0.98\mu s$. The delay power spectral density of the typical urban channel environment is shown in the Figure 4.3.

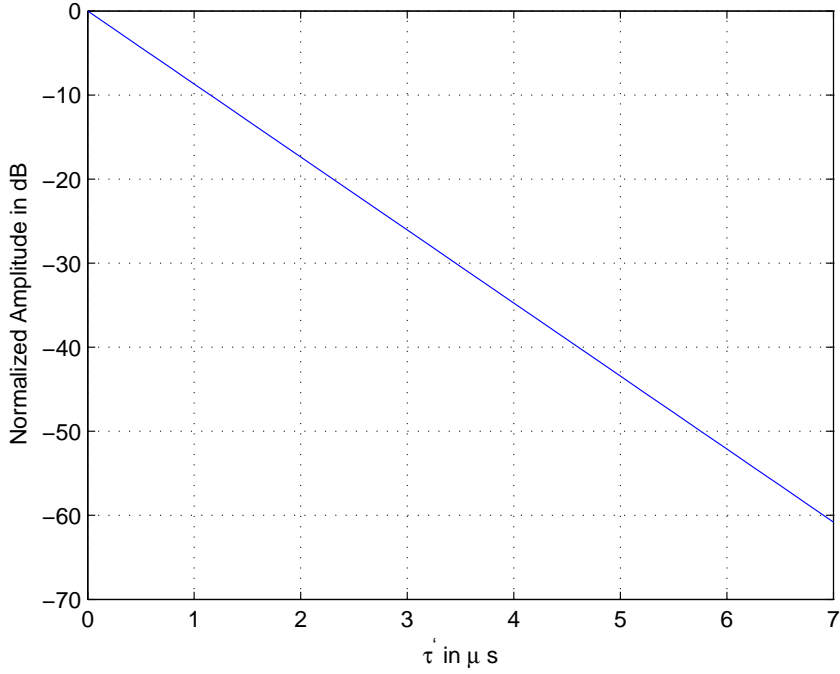


Figure 4.3: Delay power spectral density $S_{\tau'\tau'}(\tau')$ for Typical Urban (TU).

Bad Urban (BU):

$$\begin{aligned} S_{\tau'\tau'}(\tau') &= C_{BU}e^{-\tau'/\mu s}, & 0 \leq \tau' < 5\mu s \\ &= C_{BU}\frac{1}{2}e^{(5-\tau')/\mu s}, & 5 \leq \tau' \leq 15\mu s \\ &= 0, & else, \end{aligned} \quad (4.6)$$

where the real valued coefficient C_{BU} is given by

$$C_{BU} = \frac{2}{3(1 - e^{-5})} , \quad (4.7)$$

the delay spread for the Bad Urban channel model $B_{\tau'\tau'}^{(2)} = 2.53\mu s$. Figure 4.4 depicts the delay power spectral density of typical bad urban channel.

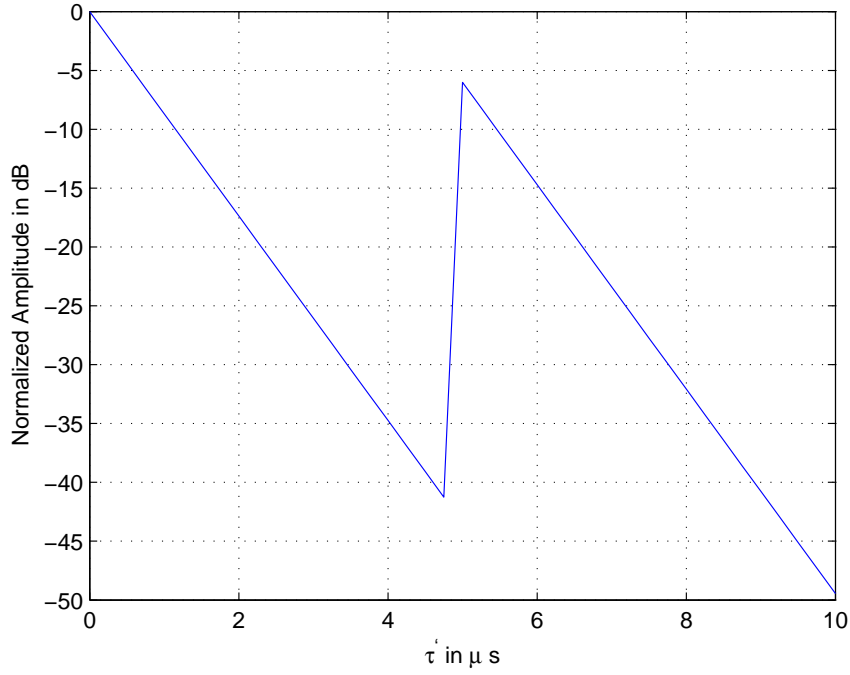


Figure 4.4: Delay power spectral density $S_{\tau'\tau'}(\tau')$ for Bad Urban Area (BU).

Hilly Terrain (HT):

$$\begin{aligned} S_{\tau'\tau'}(\tau') &= C_{HT}e^{-3.5\tau'/\mu s}, & 0 \leq \tau' < 2\mu s \\ &= C_{HT}0.1e^{(15-\tau')/\mu s}, & 15 \leq \tau' \leq 20\mu s \\ &= 0, & else, \end{aligned} \quad (4.8)$$

where the real valued coefficient C_{HT} is given by

$$C_{HT} = \frac{1}{(1 - e^{-5})/3.5 + (1 - e^{-5})/10} , \quad (4.9)$$

the delay spread for the Bad Urban channel model $B_{\tau'\tau'}^{(2)} = 6.88\mu s$. The delay power spectral density of a hilly terrain channel model is shown in the Figure 4.5.

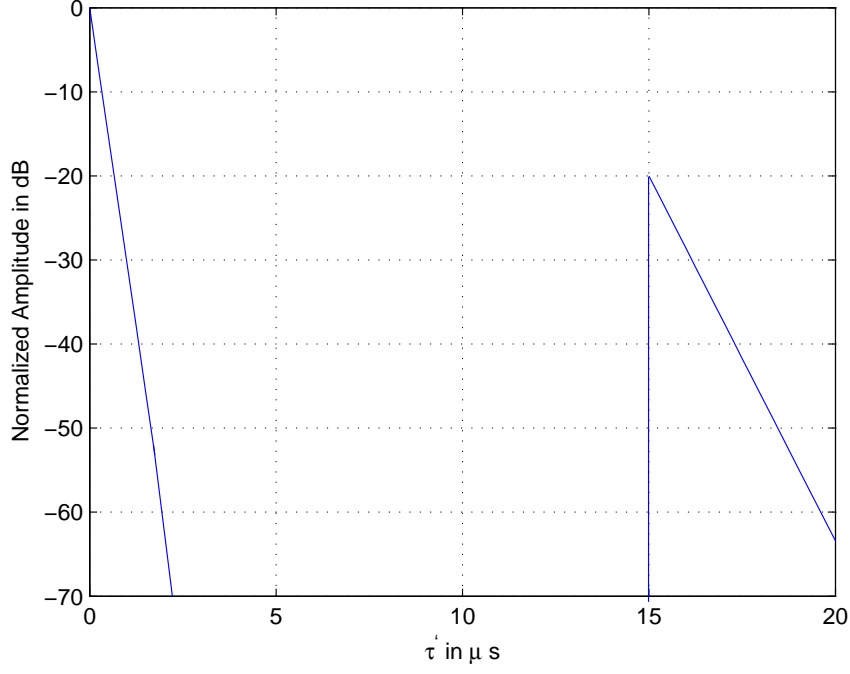


Figure 4.5: Delay power spectral density $S_{\tau'\tau'}(\tau')$ for Hilly Terrain Area (HT).

The COST 207 models specified four different Doppler power spectra $S_{\mu\mu}(f)$ defined as:

CLASS: CLASS is the classical Jakes spectrum, only occurs in case of path delays less than $500ns$, i.e., $\tau' \leq .5\mu s$, and is given by

$$S_{\mu\mu}(f) = \frac{1}{\pi f_m \sqrt{1 - (\frac{f}{f_m})^2}}, \quad |f| \leq f_m \quad (4.10)$$

where f_m represents the maximum Doppler frequency given by (1.2).

GAUS1: GAUS1 is the sum of two Gaussian functions, occurs only in the case of path delays in the range $500ns$ to $2\mu s$, i.e., $0.5\mu s \leq \tau' < 2\mu s$ and is given by

$$S_{\mu\mu}(f) = G(A_1, -0.8f_m, 0.05f_m) + G(A_1/10, 0.4f_m, 0.1f_m) \quad (4.11)$$

where $G(A_i, f_i, s_i)$ is defined as [1]

$$G(A_i, f_i, s_i) = A_i e^{-\frac{(f-f_i)^2}{2s_i^2}} \quad (4.12)$$

where $i = 1, 2$ and the value of A_1 is given by [1]

$$A_1 = 50/(\sqrt{2\pi}3f_m) \quad (4.13)$$

GAUS2: GAUS2 is the sum of two Gaussian functions, occurs only in the case of path delays greater than $2\mu s$, i.e., $\tau' \geq 2\mu s$ and is given by

$$S_{\mu\mu}(f) = G(A_2, 0.7f_m, 0.1f_m) + G(A_2/10^{1.5}, 0.4f_m, 0.15f_m) \quad (4.14)$$

where $G(A_2, f_2, s_2)$ is given by (4.13) and the value of A_2 is given by [1]

$$A_2 = 10^{1.5}/[\sqrt{2\pi}(\sqrt{10} + 0.15)f_m] \quad (4.15)$$

RICE: RICE Doppler spectrum is obtained by combining the CLASS Doppler spectrum given by (4.10) and the line-of-sight component path, and is given by [1]

$$S_{\mu\mu}(f) = \frac{1}{\pi f_m \sqrt{1 - (\frac{f}{f_m})^2}} + 0.91\delta(f - 0.7f_m), \quad |f| \leq f_m \quad (4.16)$$

the values of A_1 and A_2 given by (4.13) and (4.15) are chosen such that the following condition is satisfied [1]:

$$\int_{-\infty}^{\infty} S_{\mu\mu}(f) df = 1. \quad (4.17)$$

4.2 Deterministic Frequency Channel Models

The time-varying impulse response of a frequency-selective deterministic channel consisting of \mathcal{L} discrete propagation paths is given by [1]

$$\tilde{c}(\tau', t) = \sum_{\ell=0}^{\mathcal{L}-1} \tilde{a}_\ell \tilde{\mu}_\ell(t) \delta(\tau' - \tilde{\tau}_\ell), \quad (4.18)$$

where \tilde{a}_ℓ is real valued and is known as the *delay coefficient*. The delay power spectral density of a frequency-selective channel is determined by the delay coefficients \tilde{a}_ℓ and the discrete propagation delays τ'_ℓ . The delay coefficient \tilde{a}_ℓ of the ℓ th discrete path is a measure of the square root of the average delay power assigned to the path. The Doppler effect occurs due to the movement of the mobile unit or receiver, causes the frequency shift in each of the delayed transmitted waves. The deterministic channel modeling introduced in the section (3.1) is used to model the Doppler effect in (4.18), using complex deterministic Gaussian processes given by [1],

$$\tilde{\mu}_\ell(t) = \tilde{\mu}_{1,\ell}(t) + \tilde{\mu}_{2,\ell}(t), \quad \ell = 0, 1, 2, \dots, \mathcal{L} - 1, \quad (4.19)$$

where $\tilde{\mu}_{i,\ell}(t)$ is given by [1]

$$\tilde{\mu}_{i,\ell}(t) = \sum_{n=1}^{N_{i,\ell}} c_{i,n,\ell} \cos(2\pi f_{i,n,\ell} t + \theta_{i,n,\ell}), \quad i = 1, 2. \quad (4.20)$$

The quantity $N_{i,\ell}$ in (4.20) represents the number of harmonic functions (if $i = 1$, real part; if $i = 2$, imaginary part) of the ℓ th discrete propagation path. The parameters $c_{i,n,\ell}$, $f_{i,n,\ell}$, and $\theta_{i,n,\ell}$ are known as the Doppler coefficients, Doppler frequencies, and Doppler phases, respectively.

The complex deterministic Gaussian processes $\tilde{\mu}_{i,\ell}(t)$ must be uncorrelated for different propagation paths, to ensure that the simulation model has same properties as an uncorrelated scattering (US) model. Due to this condition the deterministic Gaussian processes $\tilde{\mu}_\ell(t)$ and $\tilde{\mu}_\lambda(t)$ are designed, such that they are uncorrelated for $\ell \neq \lambda$, where $\ell, \lambda = 0, 1, 2, \dots, \mathcal{L} - 1$. To ensure that the deterministic Gaussian process are uncorrelated for different multipath propagation paths, the discrete Doppler frequencies $f_{i,n,\ell}$ are designed in such a way that the resulting Doppler frequency sets $\{f_{i,n,\ell}\}$ are mutually exclusive, i.e., they are disjoint for different propagation paths. The condition for uncorrelated scattering (US) propagation is given by [1]

$$f_{i,n,\ell} \neq f_{j,m,\lambda} \quad \text{for } \ell \neq \lambda \quad (4.21)$$

where $i, j = 1, 2$, $n = 1, 2, \dots, N_{i,\ell}$, $m = 1, 2, \dots, N_{j,\lambda}$, and $\ell, \lambda = 0, 1, \dots, \mathcal{L} - 1$.

The correlation properties of the complex deterministic Gaussian processes, assuming that they satisfy uncorrelated scattering condition are described as [1]

$$\begin{aligned} \lim_{T \rightarrow \infty} \frac{1}{T} \int_{-T}^T \tilde{\mu}_\ell^*(t) \tilde{\mu}_\lambda(t + \tau) dt &= \tilde{r}_{\mu_\ell \mu_\ell}, \quad \text{if } \ell = \lambda, \\ &= 0, \quad \text{if } \ell \neq \lambda, \end{aligned} \quad (4.22)$$

where $\tilde{r}_{\mu_\ell \mu_\ell}(\tau)$ is given by [1]

$$\tilde{r}_{\mu_\ell \mu_\ell}(\tau) = \sum_{i=1}^2 \tilde{r}_{\mu_{i,\ell} \mu_{i,\ell}}(\tau), \quad (4.23)$$

where the autocorrelation function $\tilde{r}_{\mu_{i,\ell} \mu_{i,\ell}}(\tau)$ is given by (3.16) and this equation holds for $i = 1, 2$ and $\ell, \lambda = 0, 1, \dots, \mathcal{L} - 1$.

The statistical behavior of the time-variant impulse response $c(\tau', t)$ is determined by the parameters $c_{i,n,\ell}$, $f_{i,n,\ell}$ and $\theta_{i,n,\ell}$. We can approximate any specified or measured scattering function, by determining the parameters in such way that the statistical properties of the deterministic simulation model match to those of the reference model. A brief explanation of the procedure used to achieve this is explained in later sections.

The time-variant impulse response is causal as it fulfils the condition,

$$\tilde{c}(\tau', t) = 0 \quad \text{for } \tau' < 0, \quad (4.24)$$

this is due to that fact that the discrete propagation delays τ' cannot be negative. The output signal $y(t)$ of the channel to any arbitrary input signal $x(t)$ can be calculated using the superposition integral (section 1.2.2) and is given by

$$y(t) = \int_{-\infty}^{\infty} c(\tau', t) x(t - \tau') d\tau' \quad (4.25)$$

by substituting the Equation (4.18) for $c(\tau', t)$, we obtain,

$$y(t) = \sum_{l=1}^{\mathcal{L}-1} \tilde{a}_l \tilde{\mu}_l(t) x(t - \tau'_l). \quad (4.26)$$

The output signal $y(t)$ given by (4.26) is obtained by, superposition of \mathcal{L} delayed versions of the input signal $x(t - \tau')$. Each delayed version of the input signal is multiplied by a complex deterministic Gaussian process $\tilde{\mu}_\ell(t)$ and a real valued delay coefficient \tilde{a}_ℓ . By equating the zeroth propagation delay time $\tilde{\tau}'_0 = 0$, [1] and defining the propagation path delay differences $\Delta\tilde{\tau}'_\ell = \tilde{\tau}'_\ell - \tilde{\tau}'_{\ell-1}$ (for all $\ell = 0, 1, \dots, \mathcal{L} - 1$), [1]. The deterministic simulation model for a frequency-selective channel can be implemented as a tapped delay line structure as shown in the figure (4.6).

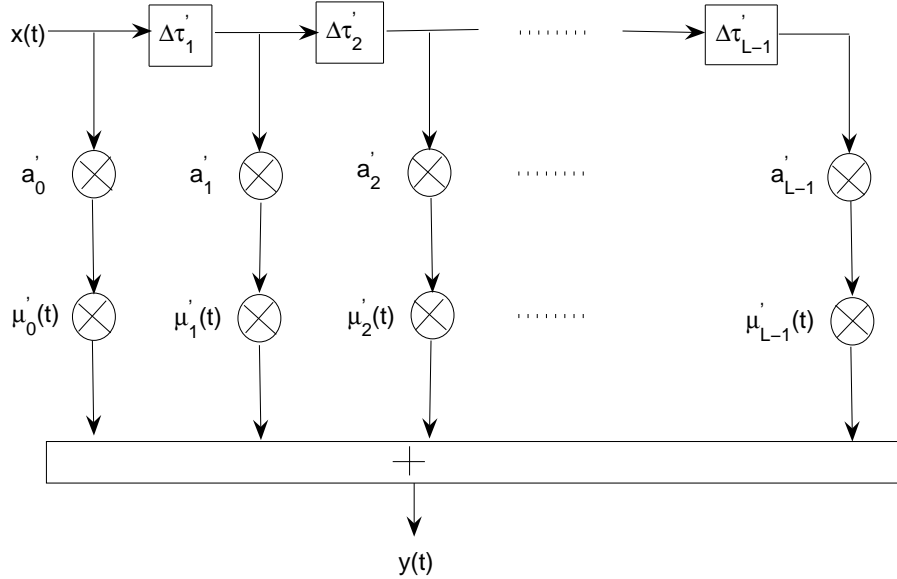


Figure 4.6: Tapped delay line model for a frequency channel model.

The simulation model, required for computer simulations is obtained from the continuous-time model, by substituting t in $x(t)$ and $y(t)$ with $t = kT'_s$ and propagation delay time $\tilde{\tau}'_\ell$ is replaced by $\tilde{\tau}'_\ell = \ell T'_s$. In the complex deterministic Gaussian process t is replaced by $t = kT_s$, where T_s and T'_s represent the sampling time periods, k is an integer and ℓ is the ℓ th propagation path. Consider the propagation path delay differences $\Delta\tilde{\tau}'_\ell = \tilde{\tau}'_\ell - \tilde{\tau}'_{\ell-1}$ by replacing the $\tilde{\tau}'_\ell = \ell T'_s$, the value of $\Delta\tilde{\tau}'_\ell = T'_s$ for all $\ell = 0, 1, \dots, \mathcal{L} - 1$. The sampling rate

T_s can be expressed in terms of T'_s as $T_s = m'_s T'_s$ where m'_s denotes the sampling rate ratio [1]. If the sampling rate ratio is large then the simulation speed is high and the error due to converting a continuous time signal $\tilde{\mu}_\ell(t)$ into discrete signal is large. The value of the sampling rate ratio m'_s is chosen in such a way that the relation $T'_s \leq T_s \leq T_{sym}$, where T_{sym} is the symbol time period, is satisfied for any given symbol interval [1]. The sampling time $T_s = T_{sym}$, if the product $f_m T_{sym}$ is very small.

Consider the time-variant transfer function given by (4.18), if all the delay amplitude coefficients are zeros excluding the zeroth coefficient i.e., $\tilde{a}_0 \neq 0, \tilde{a}_1 = \tilde{a}_2 = \dots = \tilde{a}_{\mathcal{L}-1} = 0$. This is due to fact that the obstacles which cause the scattering are far off from the receiver and the scattered components from these obstacles can be ignored. The linear-time variant transfer function given by (4.18) reduces to,

$$c(\tau', t) = \tilde{a}_0 \cdot \tilde{\mu}(t) \cdot \delta(\tau') \quad (4.27)$$

the output signal $y(t)$ of the channel to an input signal $x(t)$ given by (4.26) reduces to

$$y(t) = \tilde{\mu}(t) \cdot x(t), \quad (4.28)$$

by comparing (4.28) with (2.19), it can be concluded that the channel is frequency-nonselective.

Consider a case when there is no relative movement between the transmitter and receiver, the maximum Doppler frequency f_m given by (1.2) is zero, i.e., $f_m = 0$. The channel has no Doppler effect, due to this the deterministic Gaussian processes $\tilde{\mu}_\ell(t)$ are reduced to complex-valued constants represented as $\tilde{\mu}_\ell$ for all discrete propagation paths $\ell = 0, 1, \dots, \mathcal{L} - 1$. The linear time-variant transfer function given by (4.18), reduces to a time-invariant finite impulse response filter (FIR) with \mathcal{L} complex valued coefficients and is given by

$$c(\tau', t) = \sum_{\ell=0}^{\mathcal{L}-1} \tilde{a}_\ell \tilde{\mu}_\ell \delta(\tau' - \tilde{\tau}_\ell). \quad (4.29)$$

4.3 Autocorrelation Function and Power Spectral Density

In this section we present the autocorrelation and the power spectral density functions for the linear time-variant system given by (4.18). The autocorrelation function of the time-variant deterministic impulse response $\tilde{c}(\tau', t)$ is defined as [1]

$$\tilde{r}_{cc}(\tau'_1, \tau'_2; t, t + \tau) = \lim_{T \rightarrow \infty} \frac{1}{2T} \int_{-T}^T \tilde{c}^*(\tau'_1, t) \tilde{c}(\tau'_2, t + \tau) dt. \quad (4.30)$$

by substituting the expression for $\tilde{c}(\tau', t)$ given by (4.18) into (4.30) the expression for autocorrelation function can be written as [1]

$$\tilde{r}_{cc}(\tau'_1, \tau'_2; t, t + \tau) = \lim_{T \rightarrow \infty} \frac{1}{2T} \int_{-T}^T \left[\sum_{\ell=0}^{\mathcal{L}-1} \tilde{a}_\ell \tilde{\mu}_\ell^*(t) \delta(\tau'_1 - \tilde{\tau}'_\ell) \right] \cdot \left[\sum_{\lambda=0}^{\mathcal{L}-1} \tilde{a}_\lambda \tilde{\mu}_\lambda(t) \delta(\tau'_2 - \tilde{\tau}'_\lambda) \right] dt, \quad (4.31)$$

by using the uncorrelated scattering condition, which states that complex deterministic processes $\tilde{\mu}_\ell(t)$ are uncorrelated for different propagation paths, the equation (4.31) reduces to

$$\tilde{r}_{cc}(\tau'_1, \tau'_2; t, t + \tau) = \sum_{\ell=0}^{\mathcal{L}-1} \tilde{a}_\ell^2 \tilde{r}_{\mu_\ell \mu_\ell}(\tau) \delta(\tau'_1 - \tilde{\tau}'_\ell) \delta(\tau'_2 - \tilde{\tau}'_\ell). \quad (4.32)$$

In the equation (4.32) the product of two delta functions $\delta(\tau'_1 - \tilde{\tau}'_\ell) \delta(\tau'_2 - \tilde{\tau}'_\ell)$ is equivalent to $\delta(\tau'_1 - \tilde{\tau}'_\ell) \delta(\tau'_2 - \tilde{\tau}'_1)$, by substituting this relation, the equation (4.32) can be represented as [1]

$$\tilde{r}_{cc}(\tau'_1, \tau'_2; t, t + \tau) = \delta(\tau'_2 - \tilde{\tau}'_1) \tilde{S}_{cc}(\tau'_1, \tau), \quad (4.33)$$

where $\tilde{S}_{cc}(\tau'_1, \tau)$ denotes the *delay cross-power spectral density* of the frequency selective deterministic channel models and is given by [1]

$$\tilde{S}_{cc}(\tau', \tau) = \sum_{\ell=0}^{\mathcal{L}-1} \tilde{a}_\ell^2 \tilde{r}_{\mu_\ell \mu_\ell}(\tau) \delta(\tau' - \tilde{\tau}'_\ell). \quad (4.34)$$

In the equation (4.33) if $\tau'_2 = \tilde{\tau}'_1$, then $\tilde{r}_{cc}(\tau'_1, \tau'_2; t, t + \tau) = \tilde{S}_{cc}(\tau'_1, \tau)$, and if the condition is not true i.e., if $\tau'_2 \neq \tilde{\tau}'_1$, then $\tilde{r}_{cc}(\tau'_1, \tau'_2; t, t + \tau) = 0$. From the explanation given above

it is clear that, complex deterministic processes are uncorrelated for different propagation paths. The scattering function $\tilde{S}(\tau', f)$ of the time-variant deterministic impulse response given by (4.18) is obtained by taking the Fourier transform of delay cross-power spectral density $\tilde{S}_{cc}(\tau', \tau)$ and is given by [1]

$$\tilde{S}(\tau', f) = \sum_{\ell=0}^{\mathcal{L}-1} \tilde{a}_{\ell}^2 \tilde{S}_{\mu_{\ell}\mu_{\ell}}(f) \delta(\tau' - \tilde{\tau}_{\ell}'), \quad (4.35)$$

where $\tilde{S}_{\mu_{\ell}\mu_{\ell}}(f)$ in (4.35) represents the scattering function of the ℓ th scattering component and is given by [1]

$$\tilde{S}_{\mu_{\ell}\mu_{\ell}}(f) = \sum_{i=1}^2 \sum_{n=1}^{N_{i,\ell}} \frac{c_{i,n,\ell}^2}{4} [\delta(f - f_{i,n,\ell}) + \delta(f + f_{i,n,\ell})], \quad \ell = 0, 1, \dots, \mathcal{L} - 1. \quad (4.36)$$

The scattering function given by (4.35) can be represented by a finite sum of weighted delta functions. It is assumed that the volume under scattering function $\tilde{S}(\tau', f)$ is equal to one, i.e., [1]

$$\int_{-\infty}^{\infty} \int_0^{\infty} \tilde{S}(\tau', f) d\tau' df = 1. \quad (4.37)$$

For this assumption to be true, the Doppler coefficients $c_{i,n,\ell}$ and the delay path coefficients \tilde{a}_{ℓ} must satisfy the boundary conditions i.e.,

$$\sum_{n=1}^{N_{i,\ell}} c_{i,n,\ell}^2 = 1 \quad (4.38)$$

and

$$\sum_{\ell=0}^{\mathcal{L}-1} \tilde{a}_{\ell}^2 = 1. \quad (4.39)$$

4.4 Determination of Model Parameters

To approximate a given or measured scattering function, the model parameters must be realized in such a way that the simulation model approximates the statistical properties of the referenced model very closely. In this section we present methods to realize the model parameters $\tilde{\tau}_{\ell}'$, \tilde{a}_{ℓ} , $f_{i,n,\ell}$, $c_{i,n,\ell}$, and $\theta_{i,n,\ell}$ of the time-variant impulse response given by (4.18).

Let $S(\tau', f)$ be the given or measured scattering function, the first step is to determine the Delay power spectral density denoted as $S_{\tau'\tau'}(\tau')$ and the Doppler power spectral density $S_{\mu\mu}(f)$ which can be computed from the scattering function using the relations given below [1]

$$S_{\tau'\tau'}(\tau') = \int_{-\infty}^{\infty} S(\tau', f) df, \quad (4.40)$$

and

$$S_{\mu\mu}(f) = \int_{-\infty}^{\infty} S(\tau', f) d\tau'. \quad (4.41)$$

The delay power spectral density function $S_{\tau'\tau'}(\tau') = 0$ for values of $\tau' < 0$, this is due to that fact that the values of discrete propagation delays cannot be negative. $S_{\tau'\tau'}(\tau') = 0$ satisfies the condition given below

$$S_{\tau'\tau'}(\tau') = 0, \text{ if } \tau' > \tau'_m. \quad (4.42)$$

The next step is to get \mathcal{L} disjoint subintervals by partitioning the interval given by $I = [0, \tau']$ according to $\cup_{\ell=0}^{\mathcal{L}-1} I_\ell$ [1]. The partition has to be realized in such a way that the Delay power spectral density $S_{\tau'\tau'}(\tau')$ and the Doppler power spectral density $S_{\mu\mu}(f)$ have to be independent within each subinterval I_ℓ . The scattering function $S(\tau', f)$ is expressed as the product of Doppler power spectral density and delay power spectral density within the subinterval I_ℓ and is given by [1]

$$S(\tau', f) = \sum_{\ell=0}^{\mathcal{L}-1} S_{\mu\mu}(f) S_{\tau'\tau'}(\tau') |_{\tau' \in I_\ell}. \quad (4.43)$$

The discrete propagation path delays and the propagation coefficients are computed from (4.43). The discrete propagation path delays τ'_ℓ are obtained by sampling and are given by integer multiples of sampling time interval T'_s [1],

$$\tilde{\tau}'_\ell = \ell \cdot T'_s, \quad \ell = 0, 1, \dots, \mathcal{L} - 1 \quad (4.44)$$

the number of paths \mathcal{L} is given by [1]

$$\mathcal{L} = \lfloor \frac{\tau'_m}{T'_s} \rfloor + 1. \quad (4.45)$$

From (4.45) it is clear that the number of discrete paths \mathcal{L} are determined by the ratio τ'_m/T'_s . The subintervals required for the partition of the interval $I = [0, \tau'_m]$ are defined in [1] as follows:

$$\begin{aligned} I_\ell &= [0, T'_s), \quad \ell = 0, \\ &= [\tilde{\tau}'_\ell - T'_s/2, \tilde{\tau}'_\ell + T'_s/2), \quad \ell = 1, 2, \dots, \mathcal{L} - 2, \\ &= [\tilde{\tau}'_\ell - T'_s/2, \tau'_m], \quad \ell = \mathcal{L} - 1. \end{aligned} \quad (4.46)$$

within the subinterval the areas under the delay spectral densities $S_{\tau'\tau'}(\tau')$ and $\tilde{S}_{\tau'\tau'}(\tau')$ have to be equal [1] this condition is given by

$$\int_{\tau' \in I_\ell} \tilde{S}_{\tau'\tau'}(\tau') d\tau' = \int_{\tau' \in I_\ell} S_{\tau'\tau'}(\tau') d\tau', \quad (4.47)$$

the above condition holds for all $\ell = 0, 1, \dots, \mathcal{L} - 1$, where $\tilde{S}_{\tau'\tau'}(\tau')$ represents the deterministic delay spectral density and is given by,

$$\tilde{S}_{\tau'\tau'}(\tau') = \sum_{\ell=0}^{\mathcal{L}-1} \tilde{a}_\ell^2 \delta(\tau' - \tau'_\ell) \quad (4.48)$$

by substituting (4.38) into (4.37) we obtain the relation given by [1]

$$\tilde{a}_\ell = \sqrt{\int_{\tau' \in I_\ell} S_{\tau'\tau'}(\tau') d\tau'}, \quad \ell = 0, 1, \dots, \mathcal{L} - 1, \quad (4.49)$$

from (4.49) it is clear that the delay coefficient \tilde{a}_ℓ associated with ℓ th path is obtained from the square root of the average path power calculated within the interval I_ℓ .

To determine the simulation model parameters, to approximate the Doppler power spectral density the methods specified in the section (3.3) were used. The discrete Doppler coefficients $f_{i,n,\ell}$, the Doppler coefficients $c_{i,n,\ell}$ are computed using the method of exact Doppler spread (MEDS). The method of exact Doppler spread has been developed especially for Jakes power spectral density. In our channel simulation model we assumed the Doppler power spectral density to be CLASS (section 4.1), which is the classic Jakes power spectral density. The

complex deterministic processes $\tilde{\mu}_\ell(t)$ and $\tilde{\mu}_\lambda(t)$ must be uncorrelated for $\ell \neq \lambda$, this condition is satisfied, if the number of harmonics $N_{i,\ell}$ and $N_{j,\lambda}$ used to realize the complex deterministic Gaussian processes are different i.e., $N_{i,\ell} \neq N_{j,\lambda}$ for $\ell \neq \lambda$, where $i, j = 1, 2$ and $\ell, \lambda = 0, 1, \dots, \mathcal{L} - 1$. The discrete Doppler phases $\theta_{i,n,\ell}$ are calculated using the Doppler phase vector given by (3.39).

Chapter 5

Simulation Results

In this chapter we present the scattering functions generated for the four typical channel models according to COST 207. Consider the time-variant deterministic impulse response $\tilde{c}(\tau', t)$ of a frequency selective fading channel given by (4.18),

$$\tilde{c}(\tau', t) = \sum_{\ell=0}^{\mathcal{L}-1} \tilde{a}_{\ell} \tilde{\mu}_{\ell}(t) \delta(\tau' - \tilde{\tau}_{\ell}'). \quad (5.1)$$

The first step is to get the delay amplitude coefficients \tilde{a}_{ℓ} for the four propagation environments specified by COST 207. The Figure 5.1 depicts the power delay profile of Typical Urban (TU) propagation model specified COST 207. The Figure 5.2 depicts the power delay profile of Rural Area (RA) propagation model specified by COST 207. The amplitude delay coefficients \tilde{a}_{ℓ} are obtained by using the equation (4.48) given by

$$\tilde{a}_{\ell} = \sqrt{\int_{\tau' \in I_{\ell}} S_{\tau' \tau'}(\tau') d\tau'}, \quad \ell = 0, 1, \dots, \mathcal{L} - 1, \quad (5.2)$$

where ℓ is the ℓ th propagation path and \mathcal{L} represents the total number of propagation delay paths. The amplitude coefficients satisfy the boundary condition given by equation (4.39). The number of discrete propagation delay paths \mathcal{L} , are computed by using the equation (4.45) given by [1]

$$\mathcal{L} = \lfloor \frac{\tau_m'}{T_s'} \rfloor + 1. \quad (5.3)$$

The next step is to realize the deterministic complex Gaussian random processes $\tilde{\mu}_{\ell}(t)$ such that they approximate the Doppler power spectral densities specified by COST 207 for different propagation environments (refer to section 4.1). We assumed classic Jakes power spectral density for all channels models specified by COST 207. To realize the deterministic

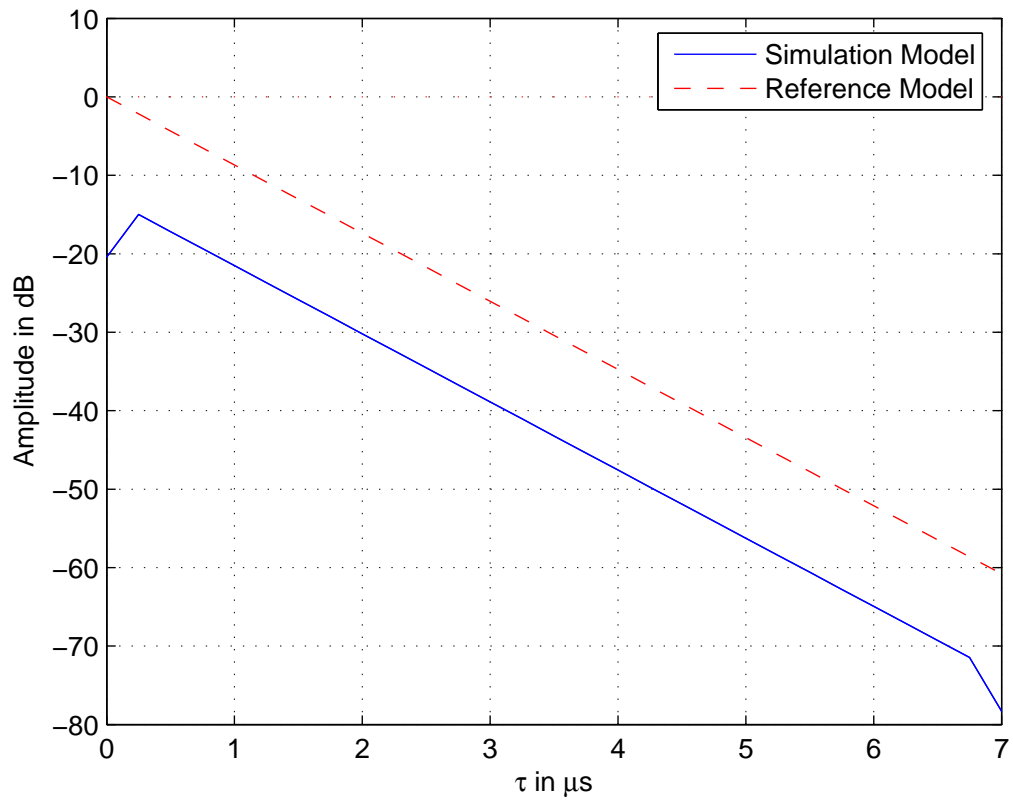


Figure 5.1: The Multipath Power Delay Profile $\tilde{S}_{\tau'\tau'}(\tau')$ of a Typical Urban power delay profile .

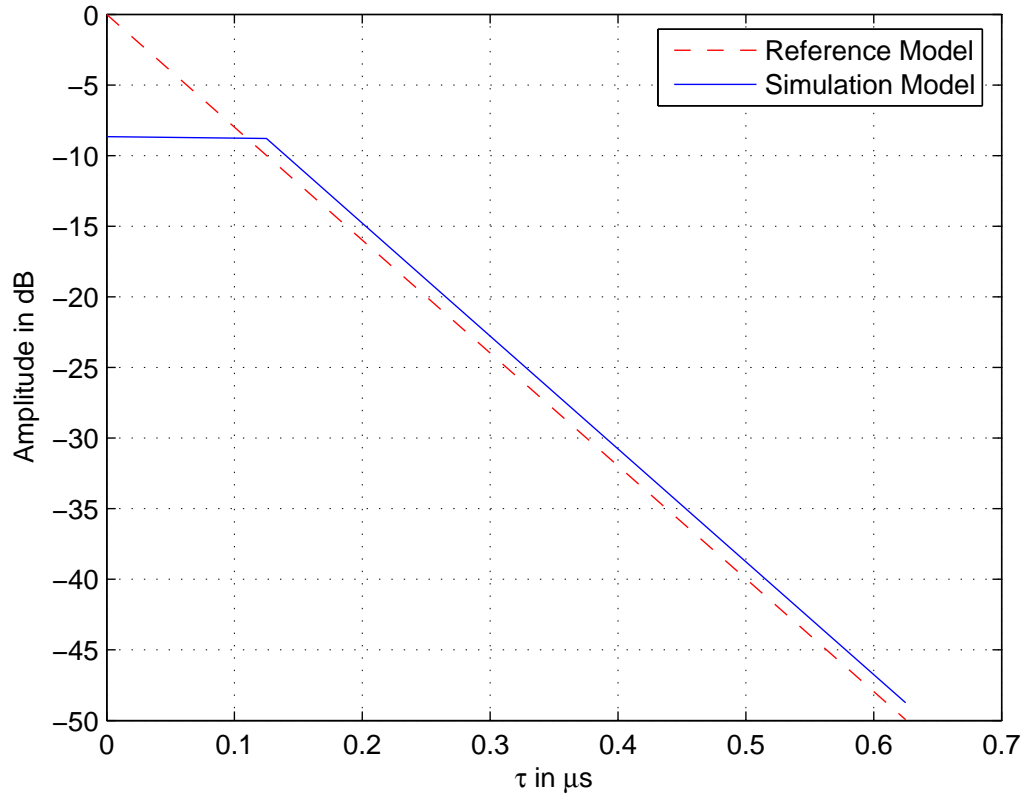


Figure 5.2: The Multipath Power Delay Profile $\tilde{S}_{\tau',\tau'}(\tau')$ of a Rural Area (RA) power delay profile .

complex Gaussian random processes $\tilde{\mu}_\ell(t)$, given by [1]

$$\tilde{\mu}_\ell(t) = \tilde{\mu}_{1,\ell}(t) + \tilde{\mu}_{2,\ell}(t), \quad \ell = 0, 1, 2, \dots, \mathcal{L} - 1, \quad (5.4)$$

where $\tilde{\mu}_{i,\ell}(t)$ in equation (5.4) is given by [1]

$$\tilde{\mu}_{i,\ell}(t) = \sum_{n=1}^{N_{i,\ell}} c_{i,n,\ell} \cos(2\pi f_{i,n,\ell} t + \theta_{i,n,\ell}), \quad i = 1, 2, \quad (5.5)$$

where $N_{i,\ell}$ is the number of harmonic functions. To realize the complex deterministic Gaussian random processes we generate the parameters of the model, Doppler coefficients $c_{i,n,\ell}$, Doppler phases $\theta_{i,n,\ell}$, Doppler frequencies $f_{i,n,\ell}$. The model parameters are computed using the method of exact Doppler spread. The Doppler coefficients $c_{i,n,\ell}$ are given by [1]

$$c_{i,n,\ell} = \sigma_0 \sqrt{\frac{2}{N_{i,\ell}}}, \quad (5.6)$$

where σ_0 is the average power. The discrete Doppler frequencies f_n given by

$$f_n = f_m \sin\left(\frac{\pi n}{2N}\right), \quad (5.7)$$

the discrete Doppler frequencies $f_{i,n,\ell}$ have to be computed in such a way that the two different propagation path signals must be uncorrelated and also the underlying real deterministic Gaussian random processes in the complex deterministic process are uncorrelated. The Doppler random phases $\theta_{i,n,\ell}$ are obtained by using equation (3.39). Once we generate all simulation parameters required to generate the time-variant deterministic impulse response we compute the autocorrelation function of the deterministic impulse response by calculating the autocorrelation function for each path. The scattering function $\tilde{S}(\tau', f)$ is obtained by computing the Fourier transform of each path's autocorrelation function weighted by square of the delay coefficient associated with that path and is given by

$$\tilde{S}(\tau', f) = \sum_{\ell=0}^{\mathcal{L}-1} \tilde{a}_\ell^2 \tilde{S}_{\mu_\ell \mu_\ell}(f) \delta(\tau' - \tilde{\tau}'_\ell). \quad (5.8)$$

5.1 Results

For all the simulations, the sampling time $T_S = 1\mu s$, the sampling rate ratio $m_s = 4$, number of harmonic functions $N = 32$, maximum Doppler frequency $f_m = 100Hz$ were used. The impulse response of a time-variant frequency selective channel is as shown in Figure 5.3. The autocorrelation function, scattering function, Jakes power spectral density, and Power delay profile of a Rural Area (RA) propagation model are shown in Figures 5.4, 5.5, 5.6, and 5.7.

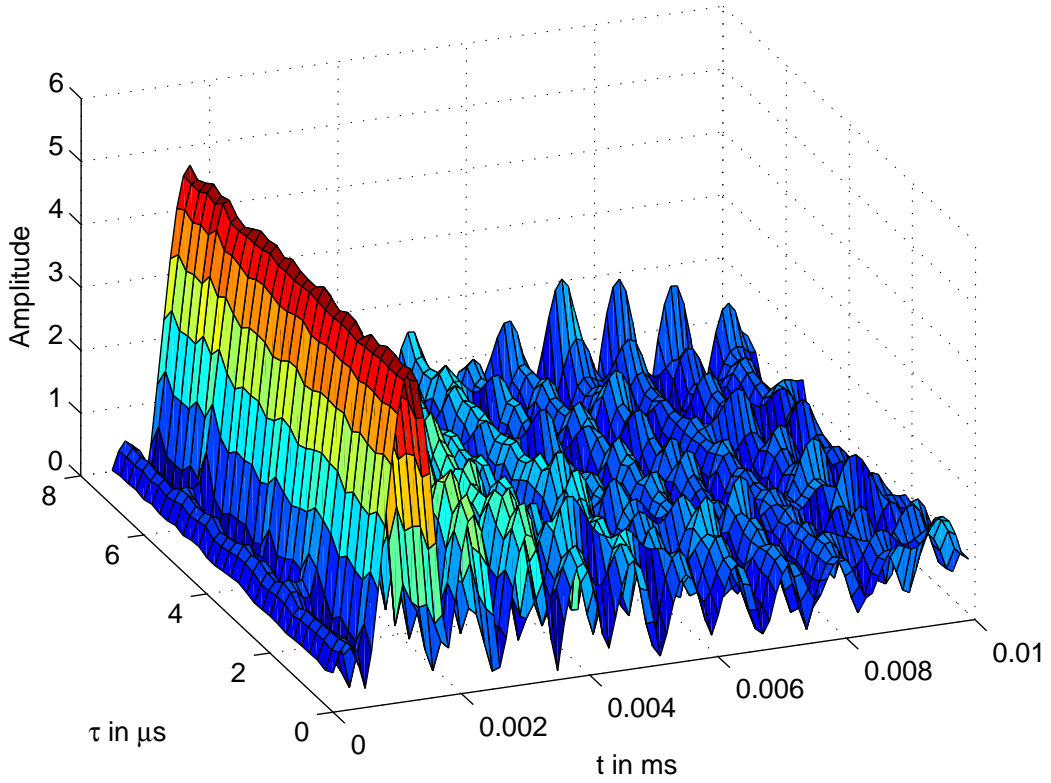


Figure 5.3: The time-variant impulse response of a frequency selective channel.

The figures from 5.7 - 5.10 show the linear time-variant impulse response, autocorrelation function, scattering function, Jakes power spectral density, power delay profile for the Typical Urban (TU) propagation model.

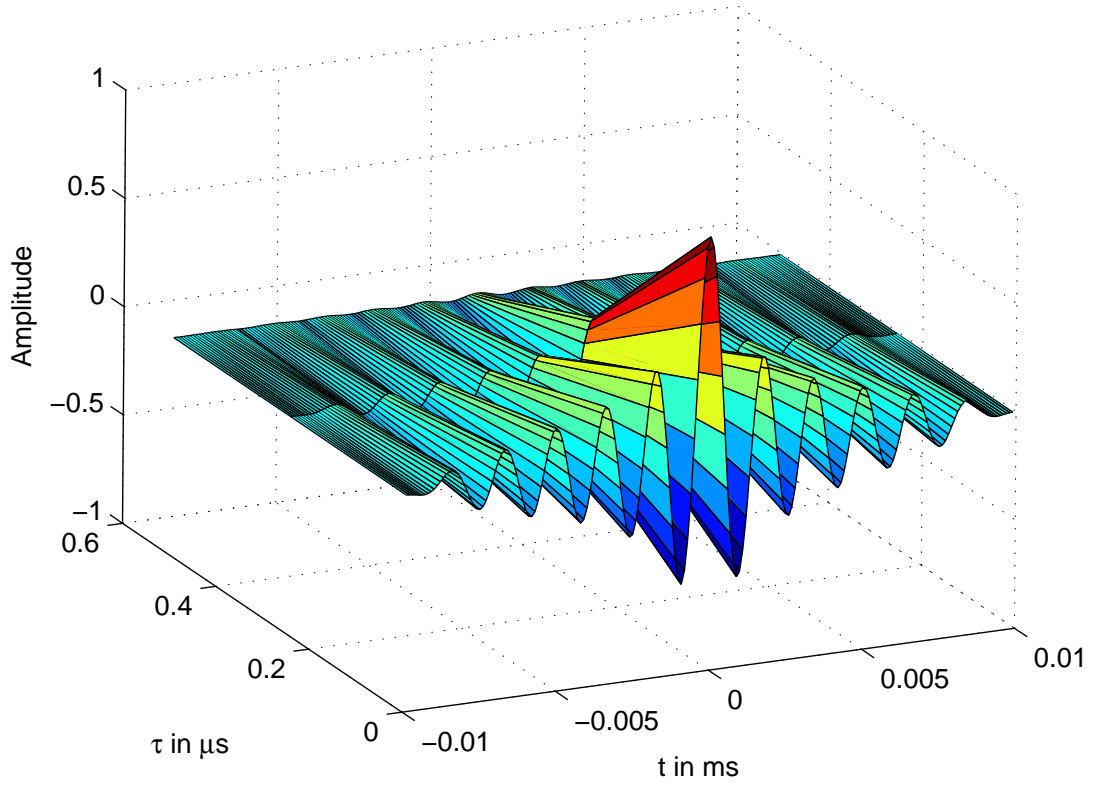


Figure 5.4: The Autocorrelation function $\tilde{r}_{\tilde{\mu}\tilde{\mu}}(\tau')$ of Rural Area propagation model.

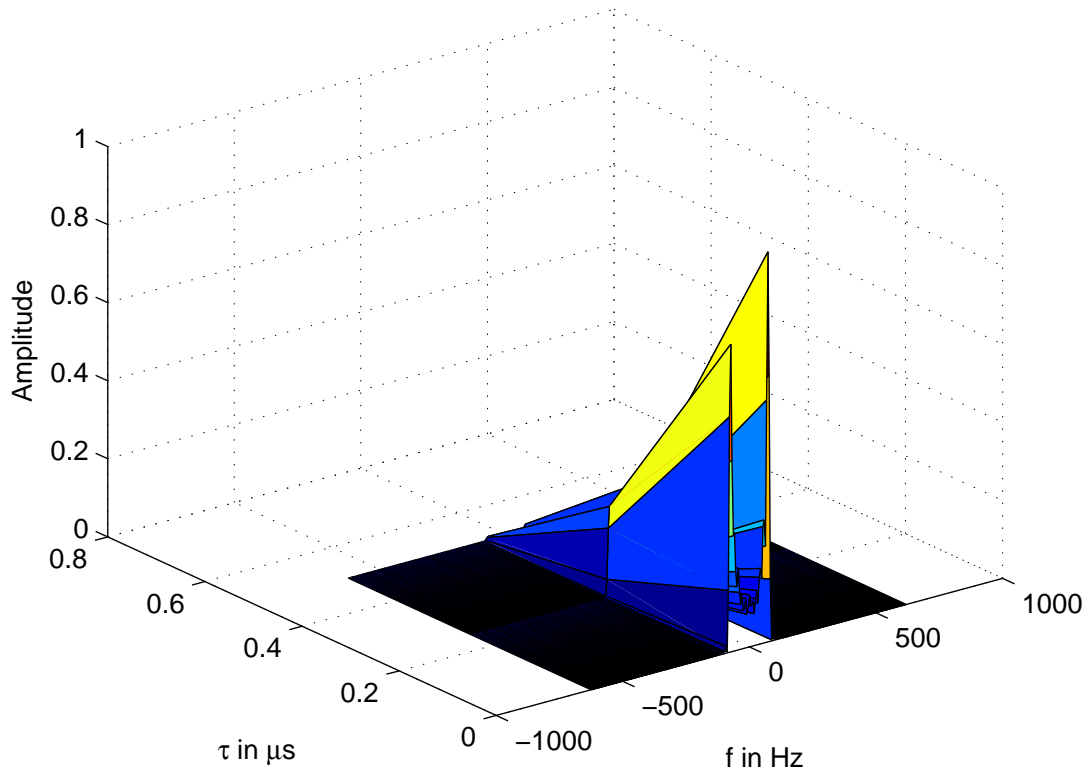


Figure 5.5: The Scattering function $\tilde{S}(\tau', f)$ of Rural Area propagation model.

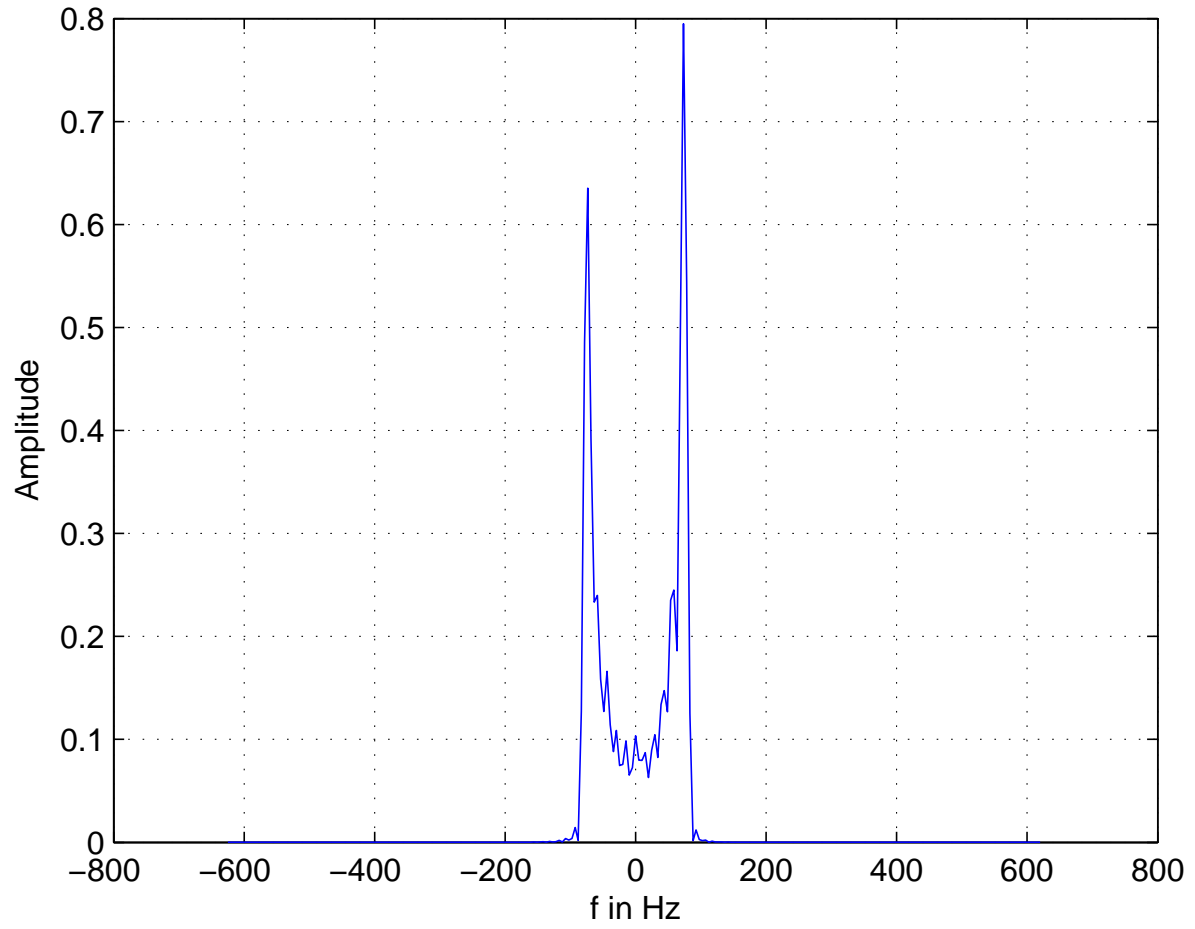


Figure 5.6: The Jakes power spectral density $\tilde{S}_{\bar{\mu}\bar{\mu}}(f)$ of Rural Area propagation model.

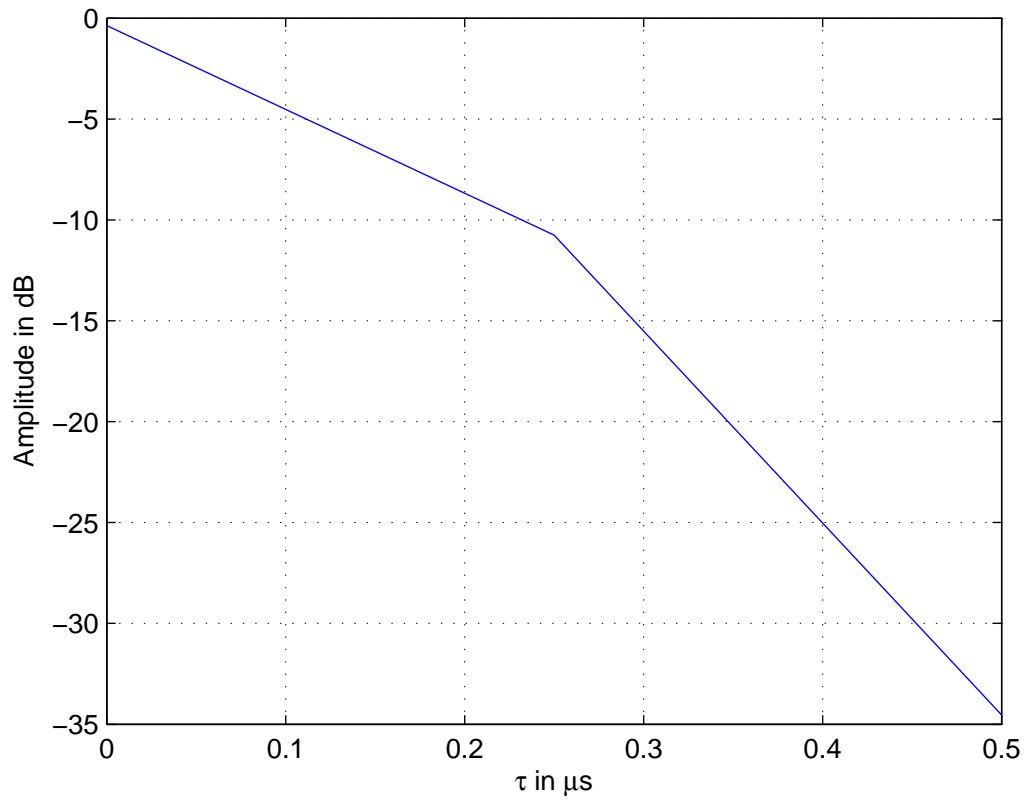


Figure 5.7: The Power Delay Profile $\tilde{S}_{\tau'\tau'}(\tau')$ of Rural Area propagation model.

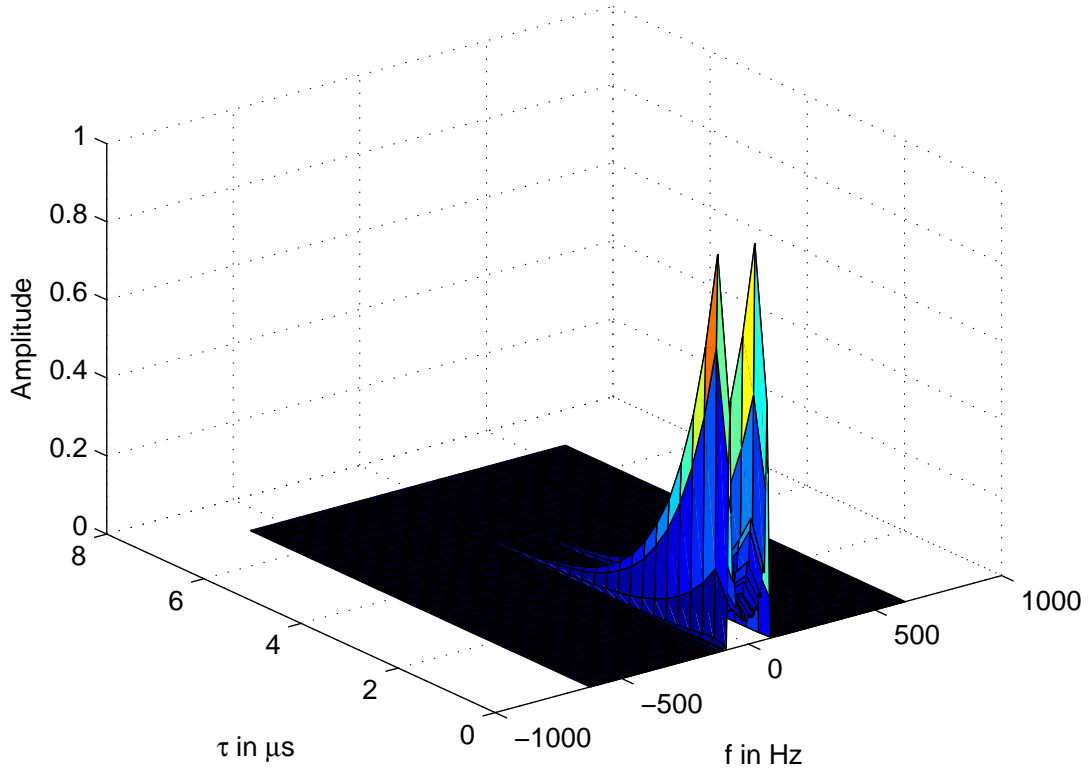


Figure 5.8: The Scattering function $\tilde{S}(\tau', f)$ of Typical Urban Area propagation model.

The figures from 5.11 - 5.13 show the scattering function, Jakes power spectral density, power delay profile for the Bad Urban (BU) propagation model.

The scattering function, power delay profile and Jakes power spectral density of a Hilly Terrain (HT) propagation model are shown in figures (5.14), (5.15), (5.16).

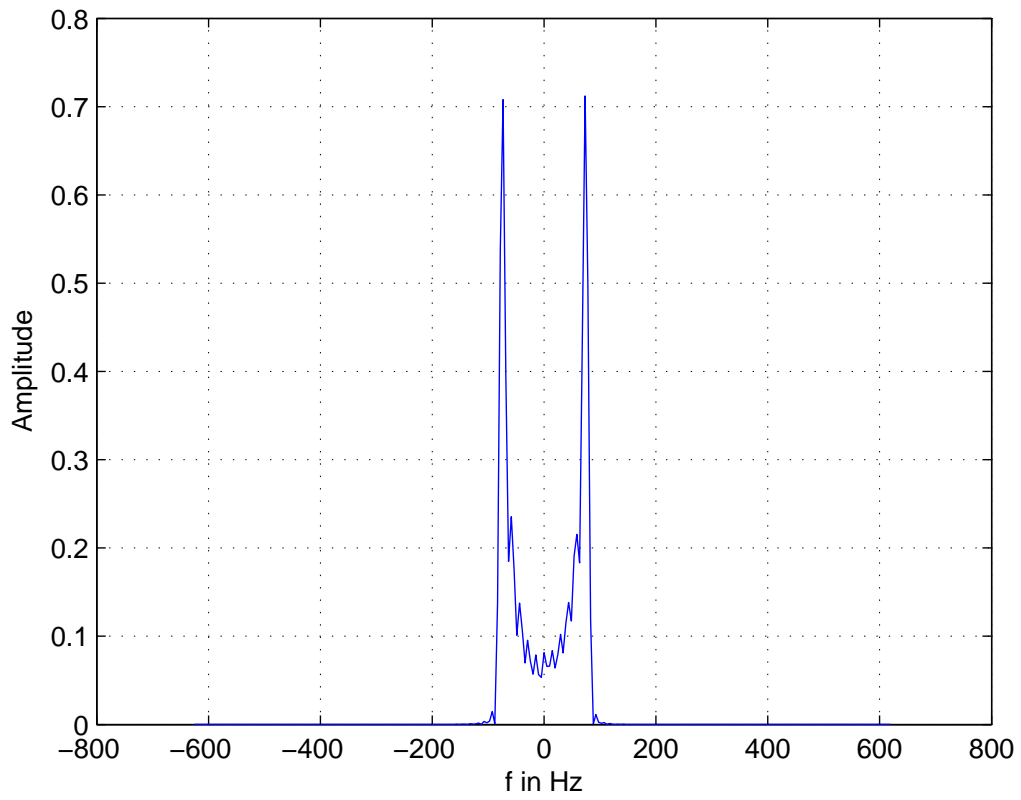


Figure 5.9: The Jakes power spectral density $\tilde{S}_{\tilde{\mu}\tilde{\mu}}(f)$ of Typical Urban Area propagation model.

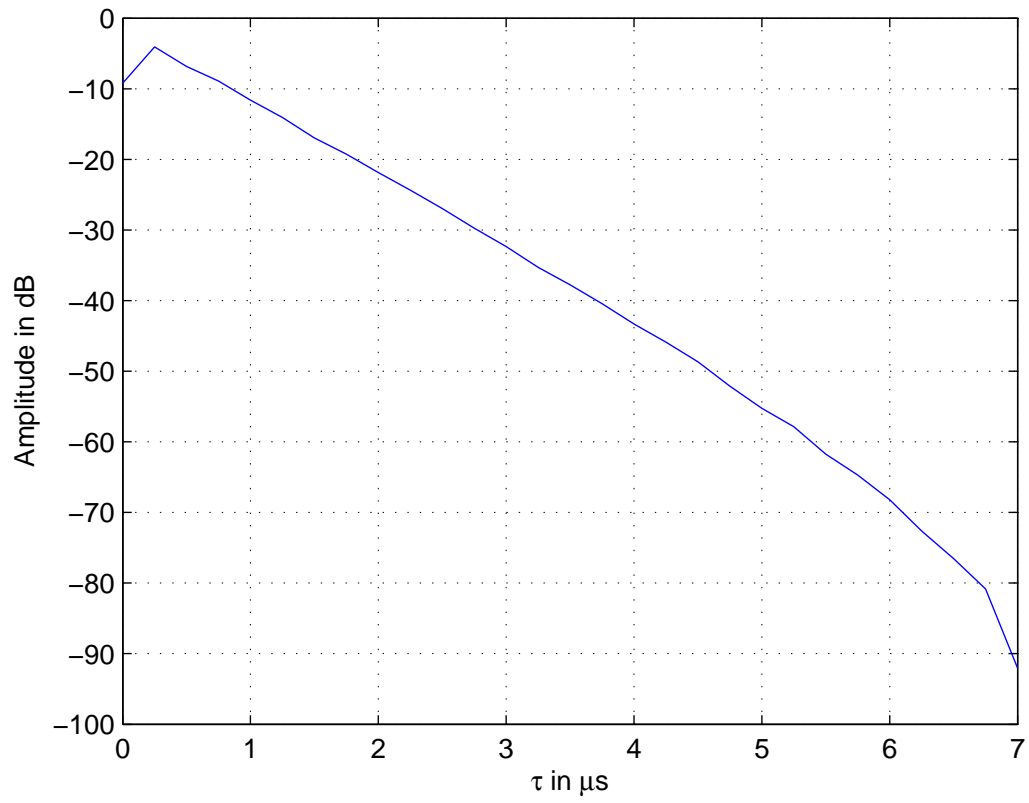


Figure 5.10: The Power Delay Profile $\tilde{S}_{\tau'\tau'}(\tau')$ of Typical Urban Area propagation model.

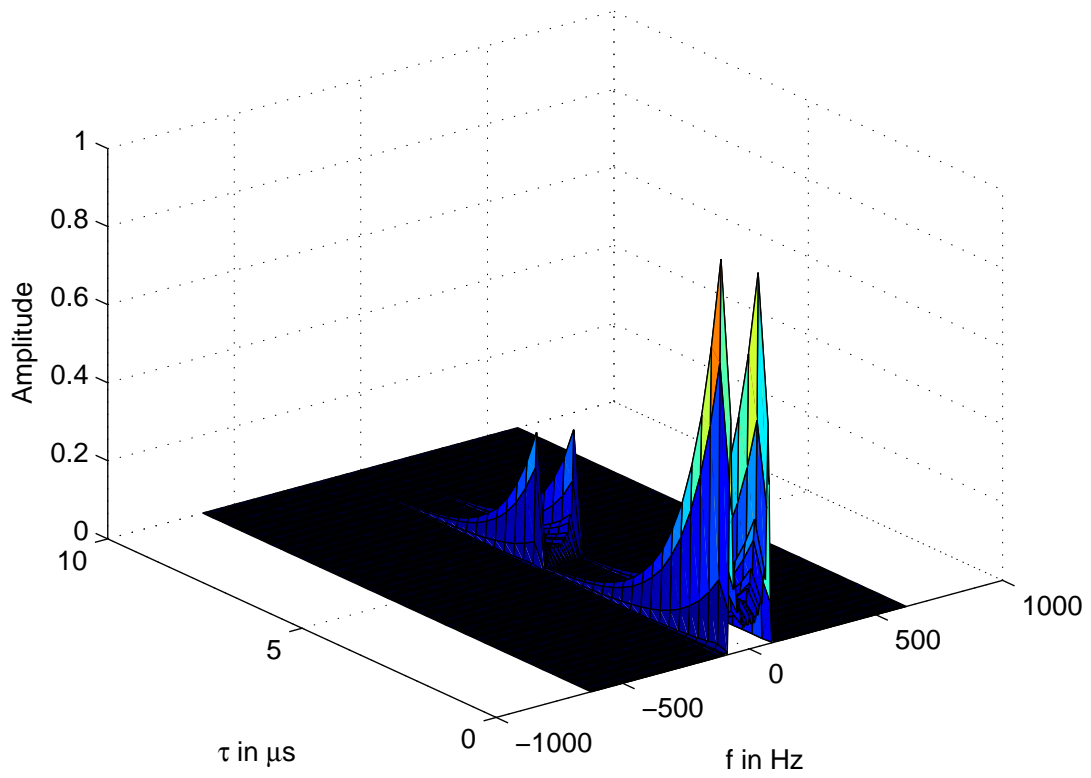


Figure 5.11: The Scattering function $\tilde{S}(\tau', f)$ of Bad Urban Area propagation model.

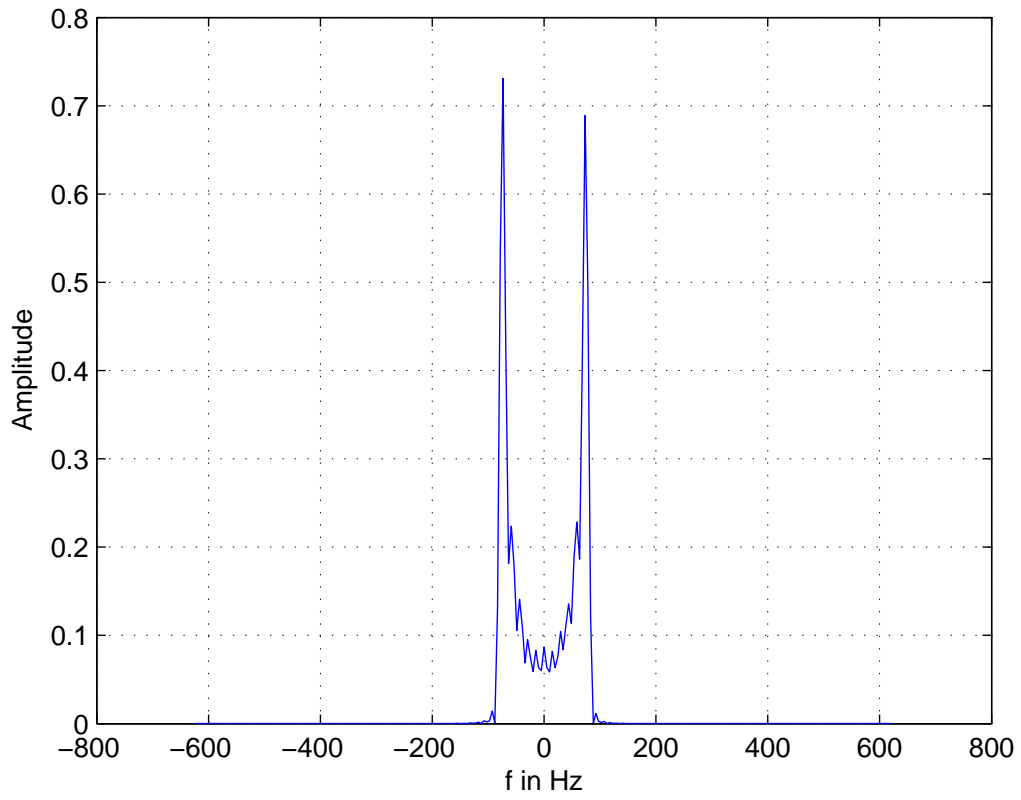


Figure 5.12: The Jakes power spectral density $\tilde{S}_{\tilde{\mu}\tilde{\mu}}(f)$ of Bad Urban Area propagation model.

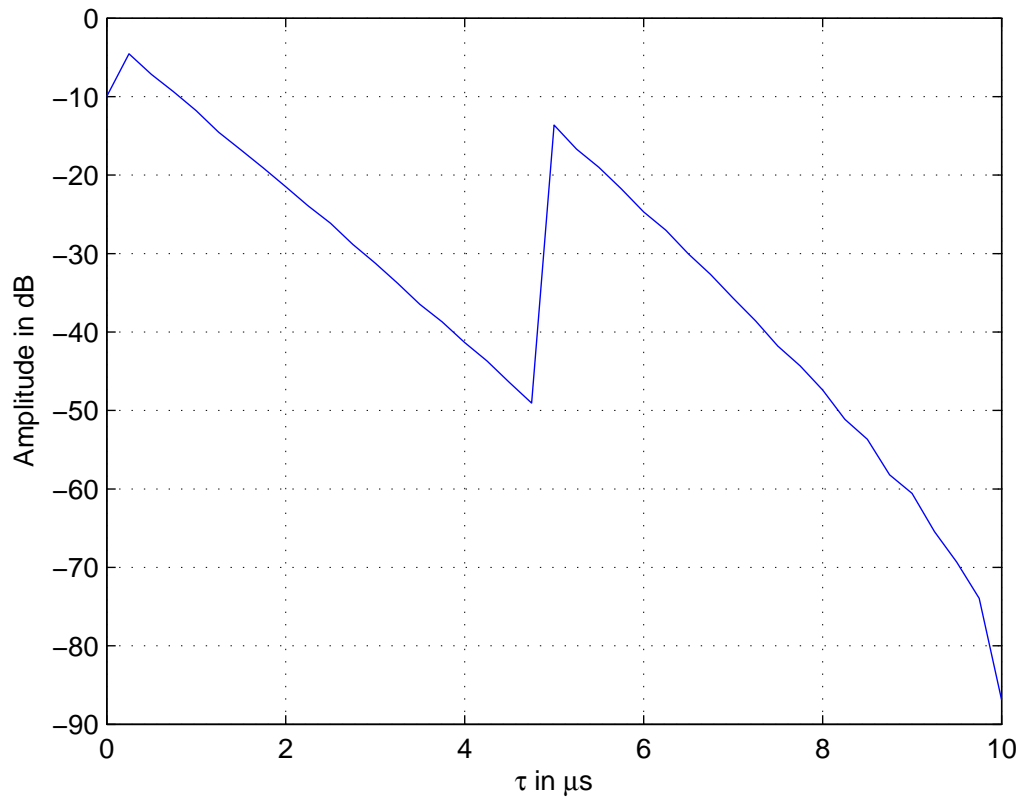


Figure 5.13: The Power Delay Profile $\tilde{S}_{\tau'\tau'}(\tau')$ of Bad Urban Area propagation model.

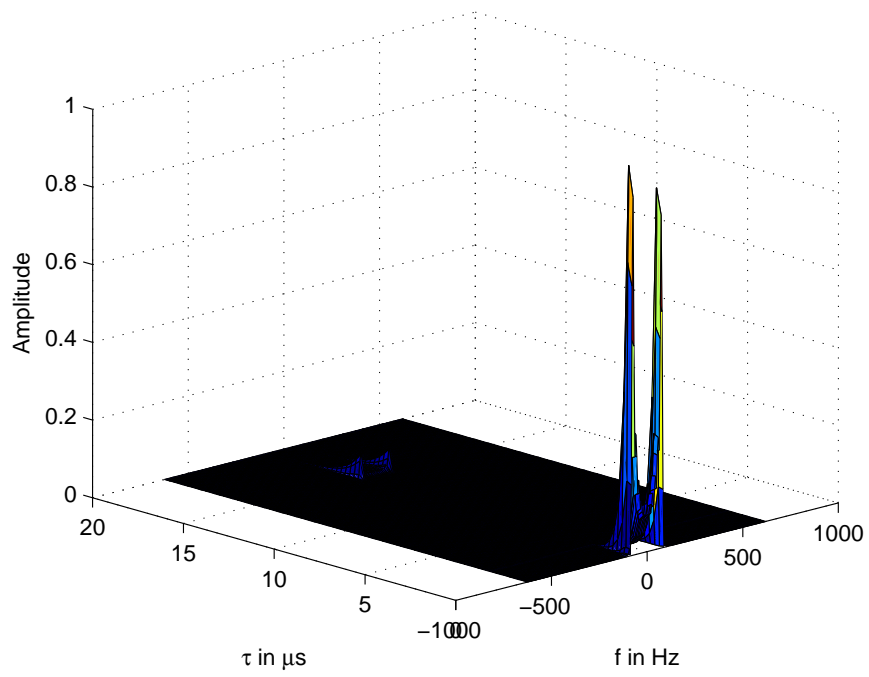


Figure 5.14: The Scattering function $\tilde{S}(\tau', f)$ of Hilly Terrain propagation model.

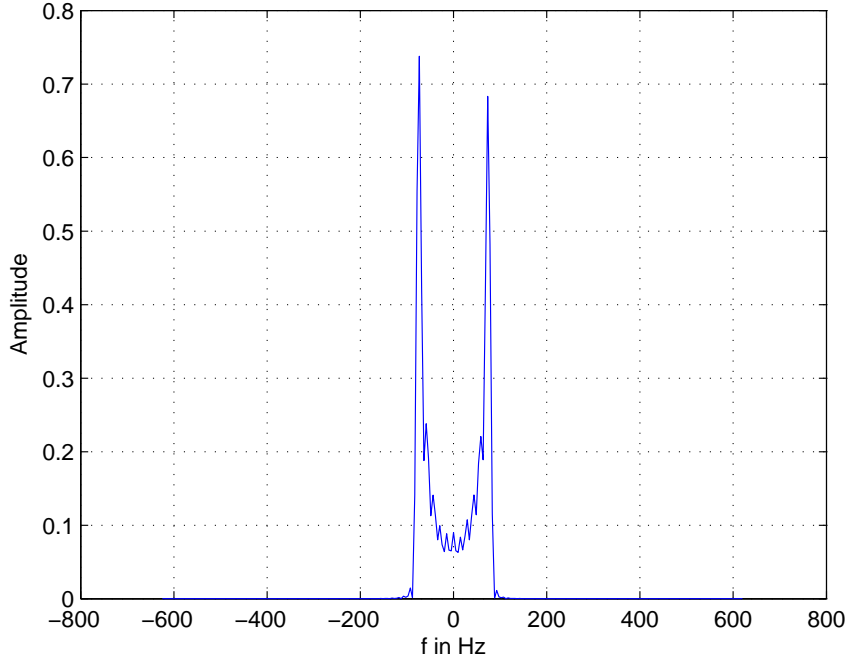


Figure 5.15: The Jakes power spectral density $\tilde{S}_{\tilde{\mu}\tilde{\mu}}(f)$ of Hilly Terrain propagation model.

5.2 Conclusion and Future Work

The frequency-selective channels were successfully simulated, scattering functions and power delay profiles were generated according to COST 207 specifications. A MATLAB simulation model which approximates the statistical properties of a reference model to model a scattering function was developed. The developed simulation model is useful to study the effects multipath fading channels and can be used to study the performance of various communication techniques in multipath fading environment.

The future work includes implementing the frequency-selective channel modeling techniques on a DSP System.

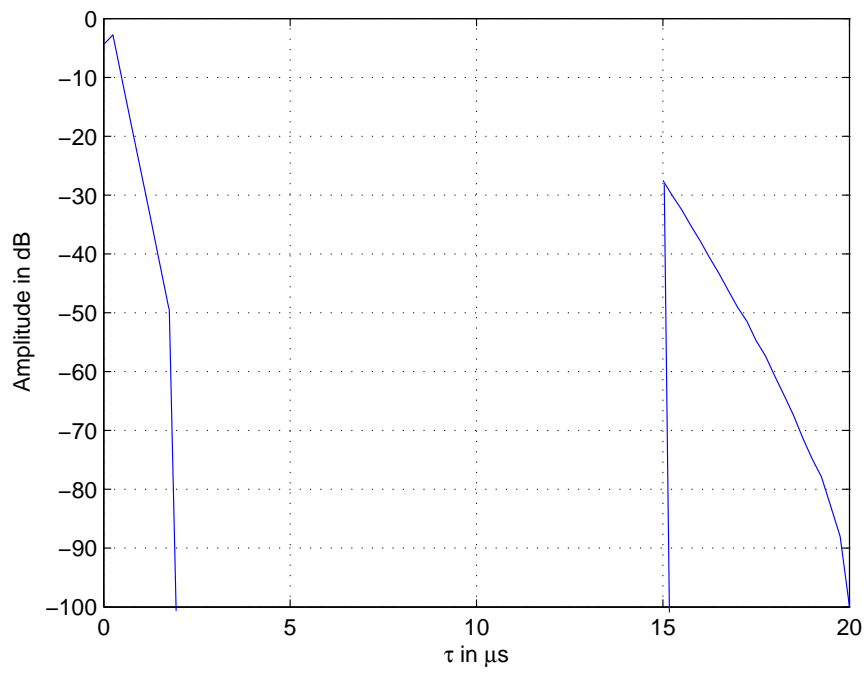


Figure 5.16: The Power Delay Profile $\tilde{S}_{\tau'\tau'}(\tau')$ of Hilly Terrain propagation model.

References

- [1] Matthias Patzold, *Mobile Fading Channels*, John Wiley and Sons, Ltd, ISBN 0-471-49549-2.
- [2] Michel C. Jeruchim, Philip Balaban, and K. Sam Shanmugan, *Simulation of Communication Systems*, Modeling, Methodology, and Techniques. Kluwer Academic/Plenum Publishers, second edition, ISBN 0-306-46267-2.
- [3] Gordon L. Stuber, *Principles of Mobile Communication*, Kluwer Academic Publishers, second edition, ISBN 0-7923-7998-5
- [4] COST 207 WG1, *Proposal on channel transfer function to be used on GSM tests late 1986*, COST 207 TD (86)51 Rev. 3, Sep. 1986.
- [5] Henry Stark, John W. Woods, *Probability and Random Processes with Applications to Signal Processing*, Prentice Hall, Upper Saddle River, NJ 07548, third edition, ISBN 0-13-020071-9.
- [6] Tao Wang, Vimal k. Dubey, and Jin Teong Ong, “Generation of Scattering Function for Mobile Communication Channel: A Computer Simulation Approach,” *International Journal of Wireless Information Networks*, Vol. 4, No. 3, pp. 187–204, 1997.
- [7] Donlad G. Childers, *Probability and Random Processes*, using matlab with applications to continuous and discrete time systems. Irwin publishers, first edition, ISBN 0-256-23803-0.
- [8] B. Sklar, “Rayleigh fading channels in mobile radio communications, Part I and II,” *IEEE communications magazine*, volume 35, issue 7, pp. 90–100, July 1997.

- [9] Yahong R. Zheng and Chengshan Xiao, "Improved Models for Generation of Multiple Uncorrelated Rayleigh Fading Waveforms," IEEE Communications Letters, Volume 6, No.6, June 2002.
- [10] R. H. Clarke, "A statistical theory of mobile-radio reception," Bell systems, Technological Journal, pp. 957-1000, July-Aug. 1968.
- [11] P. Dent, G. E. Bottomley, and T. Croft, "Jakes fading model revisited," Electronics Letters, Vol 29, no. 13, pp. 1162-1163, June 1993.
- [12] M.F. Pop and N.C. Beaulieu, "Limitations of sum-of-sinusoids fading channel simulators," IEEE Transactions on Communications, Volume 49, pp. 699-708, Apr. 2001.
- [13] Y. X. Li and X. Huang, "The generation of independent Rayleigh faders," Proceedings IEEE ICC'00, pp. 41-45, 2000.
- [14] Simon Haykin, Micheal Moher, *Modern Wireless Communications*, Pearsom Education Upper Saddle River, Nj, 07548, first edition, ISBN 0-13-022472.
- [15] Mathias Patzold, Arkadius Szczepanski, Neji Yuossef, "Methods for Modeling of Specified and Measured Multipath Power-Delay Profiles," IEEE Transactions on Vehicular Technology, Volume 51, NO. 5, September 2002.
- [16] J. D. Parsons and A. S. Bajwa, "Wideband charecterization of the fading mobile radio channels," Inst. Elec. Eng. Proc., volume 129, No. 2, pp. 95-101, April 1982.

Curriculum Vitae

Sashi Kanth Dharmannola was born on December 11th, 1982 in Hyderabad, Andhra Pradesh, India, the eldest son of Venkat Reddy Dharmannola and Srilatha Dharmannola. He graduated from Jawahar Lal Technological University (JNTU), Andhra Pradesh, India with a bachelor's degree in engineering with distinction in the field of Electrical and Communications Engineering in June 2004.

He joined The University of Texas at El Paso to pursue Master's in Electrical Engineering in Fall 2004 where he began working as a research assistant under Dr. Bryan E. Usevitch in the field of wireless communications.

Permanent address:

2-106, Ramanthapur,
Hyderabad 500013
Andhra Pradesh, India